

CENTRAL RESEARCH LIBRARY
DOCUMENT COLLECTION

CENTRAL RESEARCH LIBRARY
DOCUMENT COLLECTION

LIBRARY LOAN COPY

DO NOT TRANSFER TO ANOTHER PERSON

If you wish someone else to see this document,
send in name with document and the library will
arrange a loan.

ORNL-1164
Progress
ga



3 4456 0360925 4

PHYSICS DIVISION
QUARTERLY PROGRESS REPORT

FOR PERIOD ENDING SEPTEMBER 20, 1951



OAK RIDGE NATIONAL LABORATORY
OPERATED BY
CARBIDE AND CARBON CHEMICALS COMPANY
A DIVISION OF UNION CARBIDE AND CARBON CORPORATION



POST OFFICE BOX P
OAK RIDGE, TENNESSEE

ORNL-1164

This document consists of 66 pages.

Copy 9 of 316 copies. Series A.

Contract No. W-7405, eng 26

PHYSICS DIVISION
QUARTERLY PROGRESS REPORT
for Period Ending September 20, 1951

A. H. Snell, Director
E. O. Wollan, Associate Director

Edited by
C. G. Shull

DATE ISSUED

APR 14 1952

OAK RIDGE NATIONAL LABORATORY
Operated by
CARBIDE AND CARBON CHEMICALS COMPANY
A Division of Union Carbide and Carbon Corporation
Post Office Box P
Oak Ridge, Tennessee



3 4456 0360925 4

INTERNAL DISTRIBUTION

- | | | | |
|--------|-------------------------|--------|----------------------|
| 1. | G. T. Felbeck (C&CCC) | 34. | J. A. Lane |
| 2-3. | Chemistry Library | 35. | R. N. Lyon |
| 4. | Physics Library | 36. | W. C. Koehler |
| 5. | Biology Library | 37. | W. K. Ergen |
| 6. | Health Physics Library | 38. | E. P. Blizzard |
| 7. | Metallurgy Library | 39. | M. E. Rose |
| 8-9. | Training School Library | 40. | G. E. Boyd |
| 10-13. | Central Files | 41. | Lewis Nelson |
| 14. | C. E. Center | 42. | R. W. Stoughton |
| 15. | C. E. Larson | 43. | C. E. Winters |
| 16. | W. B. Humes (K-25) | 44. | W. H. Jordan |
| 17. | W. D. Lavers (Y-12) | 45. | E. C. Campbell |
| 18. | A. M. Weinberg | 46. | D. S. Billington |
| 19. | E. H. Taylor | 47. | M. A. Bredig |
| 20. | E. D. Shipley | 48. | R. S. Livingston |
| 21. | E. J. Murphy | 49. | C. P. Keim |
| 22. | F. C. VonderLage | 50. | J. L. Meem |
| 23. | A. H. Snell | 51. | C. E. Clifford |
| 24. | J. A. Swartout | 52. | G. H. Clewett |
| 25. | A. Hollaender | 53. | C. D. Susano |
| 26. | K. Z. Morgan | 54. | C. J. Borkowski |
| 27. | F. L. Steahly | 55. | M. J. Skinner |
| 28. | M. T. Kelley | 56. | L. A. Rayburn |
| 29. | E. M. King | 57. | S. Bernstein |
| 30. | E. O. Wollan | 58. | P. M. Reyling |
| 31. | D. W. Cardwell | 59. | D. D. Cowen |
| 32. | A. S. Householder | 60-73. | Central Files (O.P.) |
| 33. | L. D. Roberts | | |

EXTERNAL DISTRIBUTION

- 74-316. Given distribution as shown in TID 4500 under Physics Category.

Physics Division quarterly progress reports previously issued in this series are as follows:

ORNL-325 supplement	December, January, and February, 1948-1949
ORNL-366	Period Ending June 15, 1949
ORNL-481	Period Ending September 25, 1949
ORNL-577	Period Ending December 15, 1949
ORNL-694	Period Ending March 15, 1950
ORNL-782	Period Ending June 15, 1950
ORNL-865	Period Ending September 20, 1950
ORNL-940	Period Ending December 20, 1950
ORNL-1005	Period Ending March 20, 1951
ORNL-1092	Period Ending June 20, 1951

PUBLICATIONS

"Irreversibility and Generalized Noise" by H. B. Callen and T. A. Welton, *Phys. Rev.* **83**, 34-40 (1951).

"Internal Conversion Coefficients. I: The K-Shell" by M. E. Rose, G. H. Goertzel, B. I. Spinrad, J. Harr, and P. Strong, *Phys. Rev.* **83**, 79-87 (1951).

"Effect of Finite Nuclear Size in Beta Decay" by M. E. Rose and D. K. Holmes, *Phys. Rev.* **83**, 190-191 (1951).

"Neutron Diffraction by Paramagnetic and Antiferromagnetic Substances" by C. G. Shull, W. A. Strauser, and E. O. Wollan, *Phys. Rev.* **83**, 333-345 (1951).

"Relative Phase of the Interaction Constants for Mixed Invariants in Beta Decay" by L. C. Biedenharn and M. E. Rose, *Phys. Rev.* **83**, 459 (1951).

"Angular Correlation in the Triple-Cascade Transitions" by L. C. Biedenharn, G. B. Arfken, and M. E. Rose, *Phys. Rev.* **83**, 586-593 (1951).

"Thermal-Neutron-Capture Cross Sections" by H. Pomerance, *Phys. Rev.* **83**, 641-645 (1951).

"Polarization of Gamma Radiation Following Capture of Polarized Neutrons" by L. C. Biedenharn, M. E. Rose, and G. B. Arfken, *Phys. Rev.* **83**, 683 (1951).

"Neutron-Deuteron Scattering Amplitudes" by E. O. Wollan, C. G. Shull, and W. C. Koehler, *Phys. Rev.* **83**, 700-702 (1951).

"Reactions of $\text{He}^3 + \text{He}^3$ " by W. M. Good, W. E. Kunz, and C. D. Moak, *Phys. Rev.* **83**, 845-846 (1951).

TABLE OF CONTENTS

	PAGE
INTRODUCTION AND SUMMARY	1
1. SCINTILLATION SPECTROMETRY	3
Uranium Gamma-Ray Spectra	3
Uranium ²³⁵	3
Uranium ²³⁴	3
Uranium ²³⁶	5
Transition-Energy Determination for Orbital Capture	8
Measurement of Internal Conversion Coefficients of I ¹³¹	11
Gamma Rays from K ⁴⁰	12
2. ELECTRONIC DEVELOPMENT	14
Single-Channel Analyzer	14
Multichannel Analyzers	14
Discriminator-Tube Drifts	14
Scaler Improvements	15
3. SHORT-LIVED ISOMERS AND DIRECTIONAL ANGULAR CORRELATION OF SUCCESSIVE GAMMA RAYS	17
4. SHORT-PERIOD ACTIVITIES	22
Lead Isomer of 0.9-sec Half Life	22
Erbium Isomer (2.5 sec)	23
Proportional-Counter Spectrometer	24
5. HIGH-VOLTAGE ACCELERATOR PROGRAM	25
Neutron Cross Sections	25
Li ⁷ (p,n)Be ⁷ Reaction	25
Be ⁹ (p,n)B ⁹ Reaction	26
Be ⁹ (p,γ)B ¹⁰ Reaction	27
F ¹⁹ (p,γ) Reaction	30
Charged-Particle Reactions	30
Instrumental Developments	33
6. NEUTRON-DIFFRACTION STUDIES	34
Total Neutron Cross Sections at Indium Resonance	
Energy (1.44 ev)	34
Magnetic Structures of V, Cr, Cb, Mo, and W	34
Coherent antiferromagnetic reflections	35
Magnetic diffuse scattering	36
General conclusions	36
7. A CRYSTAL SPECTROMETER AS A SOURCE OF MONOENERGETIC THERMAL NEUTRONS	38
8. LOW-TEMPERATURE PHYSICS	44

	PAGE
Specific Heat of Neodymium Ethyl Sulfate and Neodymium Sulfate from 1 to 2°K	44
Theory	44
Materials used	46
Results	46
Heat-Leak Studies Below 1°K	47
9. STABLE-ISOTOPE CROSS SECTIONS	50
10. TIME-OF-FLIGHT SPECTROMETER	51
11. HEAVY-ION RESEARCH	52
Ion-Source Studies	52
Specific Ionization Studies	52
Particle Detection	52
12. STANDARD PILE	53
13. THEORETICAL PHYSICS	54
Internal Conversion Angular Correlations	54
One-Three Gamma-Gamma Angular Correlation	54
Racah-Coefficient Tabulation	54
Nuclear Polarization and Alignment	54
Inner Bremsstrahlung in Beta Decay	55
Triplet Force Between Like Nucleons	55
Angular Correlation in Neutron Decay	56
Detection of Circularly Polarized Gamma Rays	56

LIST OF FIGURES

FIGURE	TITLE	PAGE
1.1	Gamma-Ray Energy Spectrum of U^{235}	4
1.2	Comparison Between the Gamma-Ray Energy Spectrum and Alpha-Gamma-Ray Coincidences for U^{235} and U^{234}	5
1.3	Gamma-Ray Energy Spectrum of U^{234}	6
1.4	Gamma-Ray Spectra for Same Sample of U^{234} as Determined Six Days Apart	7
1.5	Gamma-Ray Energy Spectrum Obtained for an Isotopically Impure Sample of U^{236}	8
1.6	Curves Showing Presence of Fe^{55} Inner-Bremsstrahlung Radiation in Mixture of Fe^{55} and Fe^{59}	9
1.7	Continuous Gamma-Ray Spectrum of Fe^{55}	9
1.8	End-Point Energy Determination for Gamma-Ray Continuum in Fe^{55}	10
1.9	Comparison Between K^{40} Gamma-Ray Energy Spectrum and Calibration Spectra	12
1.10	Portion of Gamma-Ray Energy Spectrum of K^{40} Indicating an Upper Limit to the Amount of Annihilation Radiation Present	13
2.1	Higinbotham-Type Scaling Stage Modified to Reduce Scale-Through Errors Using High Mu Tubes	16
3.1	Gamma-Ray Spectrum from Hf^{177}	18
3.2	Angular Distribution of the Coincident Gamma Rays from Hf^{177}	19
5.1	$Li^7(p,n)Be^7$ Yield (in the Forward Direction)	26
5.2	Response of Bonner-Type Counter to Neutrons	27
5.3	$Be^9(p,n)B^9$ Yield (in the Forward Direction)	28
5.4	$Be^9(p,\gamma)B^{10}$ Yield Curve (Gamma Rays Above ~ 6 Mev)	29
5.5	$F^{19}(p,\gamma)$ Yield Curve	31
5.6	Aluminum Absorption Spectrum with Biased Proportional Counter	32
5.7	Proton Spectrum from the $He^3 + He^3$ Reaction	33

FIGURE	TITLE	PAGE
6.1	Variation of Chromium Antiferromagnetic Intensity with Temperature	36
6.2	Diffuse Neutron Scattering from Chromium and Vanadium	37
7.1	Mirror and Spectrometer Diagram	39
7.2	Intensity Reflected from Mirror as a Function of Mirror Angle	40
7.3	Intensity Reflected from Mirror and Quartz Crystal as a Function of Neutron Wavelength for Various Mirror Angles (α)	41
7.4	Total Cross Section of Indium, Gold, and Silver as a Function of Neutron Energy	42
7.5	Total Cross Section of Gold	43
7.6	Total Cross Section of Gold in the Region About the (311) Discontinuity	43
8.1	Diagram of Shield Assembly to Reduce Radiation Heat Losses to Samples at Very Low Temperatures	49

LIST OF TABLES

TABLE	TITLE	PAGE
1.1	Radiation Spectra of a Sample Containing U^{234} , U^{235} , and U^{236}	3
2.1	Plate-Current Excursions	15
3.1	Experimental Results from Lu^{177}	20
3.2	Comparison of Theoretical Conversion Coefficients with the Experimental Coefficients	20
6.1	Cross Sections at 1.44 eV	34
7.1	Total Cross Sections of Indium, Gold, and Silver at Low Neutron Energies	39
8.1	Isotopic Composition of the Neodymium Used to Prepare the Samples	46
8.2	Summary of the Specific Heat Measurements	47



INTRODUCTION AND SUMMARY

This report covers the unclassified activities of the Physics Division at Oak Ridge National Laboratory during the period June 20 to September 20, 1951. In addition to the research activities described here, the Division was pleased to sponsor, in collaboration with the Oak Ridge Institute of Nuclear Studies, a Nuclear Physics Symposium at Oak Ridge on September 13, and 14, 1951. This symposium was favored by the presence of a number of distinguished European physicists who offered contributions in their various fields of interest. Lectures by R. E. Peierls, E. Amaldi, J. Rotblat, J. Mattauich, P. Huber, and O. R. Frisch were well received by the more than 200 attendees at the symposium. On the program also were a number of presentations by Oak Ridge personnel and other American physicists, including M. E. Rose, P. R. Bell, L. I. Schiff, H. B. Willard, W. M. Good, K. Way, and J. S. Foster (McGill University). Karl Lark-Horovitz delivered a stimulating after-dinner address to conclude the conference.

In a brief summary of the research activities of the division are to be noted the following:

1. The Scintillation Spectrometry Group has reported on gamma-ray spectra from various uranium isotopes, the magnetic dipole characteristic in the 80-keV gamma ray from I^{131} by internal conversion coefficient measurement has been definitely identified, further study has been made of the gamma radiation from K^{40} , and a new method of determining K -capture transition energies by "inner bremsstrahlung" end-point measurement has been developed.

2. Electronic development on single and multichannel analyzers, discrimi-

nator-tube drifts, and scaler improvements have been studied.

3. The Re^{187} (5.5×10^{-7} sec) isomer has been classified as a magnetic dipole with some electric quadrupole transition, and studies of the angular distribution between the successive gamma rays from Hf^{177} and of the K -shell internal conversion coefficients have thrown light on the transition scheme associated with the decay of the 318-keV excited level in Hf^{177} .

4. The 0.9-sec activity in neutron-irradiated lead has been assigned to a fast-neutron reaction with Pb^{207} , and the 210-keV transition in the 2.5-sec isomer of erbium has been shown to be of $E3$ character.

5. The new 6-MeV Van de Graaff generator has been placed in operation, and a number of (p, n) , and (p, γ) reactions have been studied at the higher energy available with this machine.

6. Investigation of the $He^3 + He^3$ and the $He^3 + H^2$ reactions with the Cockcroft-Walton accelerator has continued.

7. Free-scattering cross sections for a number of nuclei and atoms have been measured by an indium absorption method, and neutron-diffraction studies on metallic chromium suggest a weak antiferromagnetic structure with a Curie temperature of about $150^\circ C$.

8. A combination mirror and diffracting-crystal arrangement has been developed to permit neutron cross-section measurements as a function of neutron energy with high resolution and without the parasitic second-order effects that are obtained with single-crystal diffraction.

9. Specific-heat studies on neodymium ethyl sulfate and neodymium sulfate have been made between 1 and 2°K which indicate a very large hyperfine structure coupling in the former, and the heat leak problems involved in the use of metal Dewar vessels at very low temperatures have been studied.

10. The neutron-capture cross sections for various stable isotopes as determined in the pile oscillator have been studied, and short progress reports on the development of a time-

of-flight neutron spectrometer, on heavy ion research, and on measurements with the standard pile have been made.

11. Brief summaries by the theoretical physics staff have been made of work concerning internal-conversion angular coefficients, one-three gamma-gamma angular correlation, nuclear polarization and alignment, inner bremsstrahlung in beta decay, triplet force between like nucleons, angular correlation in neutron decay, and detection of circularly polarized gamma rays.

PHYSICS DIVISION QUARTERLY PROGRESS REPORT

1. SCINTILLATION SPECTROMETRY

URANIUM GAMMA-RAY SPECTRA

P. R. Bell J. E. Francis
R. C. Davis M. Cassidy

The natural gamma radiations from a number of uranium isotopes have been studied by means of a scintillation spectrometer.

Uranium²³⁵. A sample of U²³⁵ containing 99.9% U²³⁵ and only 0.03% U²³⁴ was run, and some X rays and gamma rays were found. The energies and intensities are shown in Table 1.1. Figure 1.1 shows the curve obtained for the U²³⁵ sample. This curve was pieced together from a high- and a low-energy section. The uranium Y was present in this sample to equilibrium concentration. Uranium Y activities are now being run. Some of the lines in the U²³⁵ spectrum agree with the energies predicted on the basis of alpha-particle measurements reported by Ghiorso.⁽¹⁾ The agreement is not complete, however, as other gamma-ray lines are found. A coincidence measurement between the alphas and the gamma rays is being made by J. E. Francis. A parallel-plate alpha-particle chamber is used to detect the alpha particles and a scintillation counter to measure the gamma rays. The gamma-ray spectrum coincident with any alpha particle is compared with the gross gamma-ray spectrum in Fig. 1.2. The sample in use contains a considerable quantity of U²³⁴ activity, so that the gamma-ray spectrum is a sum of that from U²³⁵ and U²³⁴, as can be seen by comparing these curves with those obtained for U²³⁵ and U²³⁴. Not all

(1) A. Ghiorso, U²³⁵ Alpha Fine Structure, UCRL-1117 (Feb. 8, 1951).

TABLE 1.1

Radiation Spectra of a Sample
Containing U²³⁴, U²³⁵,
and U²³⁶

SAMPLE	ENERGY (kev)	RELATIVE INTENSITY
U ²³⁴	17 ± 2	
	53 ± 2	1.0
	93 ± 2.5	0.11 - 0.31
	118 ± 2	0.42
	[181]	
U ²³⁵	17	
	93.5 ± 2	0.89
	143 ± 3	0.22
	184 ± 3	1.0
	289 ± 5	0.12
U ²³⁶	386 ± 15	0.049
	17	
	51	
	93	
	118	
	143	
	184	
289		
	386	

of the gamma rays are found in immediate coincidence with the alpha radiation. This work is being continued using pure samples of U²³⁵ and U²³⁴ on the alpha-particle sample plates.

Uranium²³⁴. A sample of U²³⁴ containing 94.7% U²³⁴ and 4.02% U²³⁵ was measured for gamma activity as shown in Fig. 1.3. The peak at 182 kev is of the correct intensity and energy to be due to the U²³⁵ content. The low-energy pulses appear to be due to the L X rays of thorium. The

PHYSICS DIVISION QUARTERLY PROGRESS REPORT

UNCLASSIFIED
DWG.11721R1

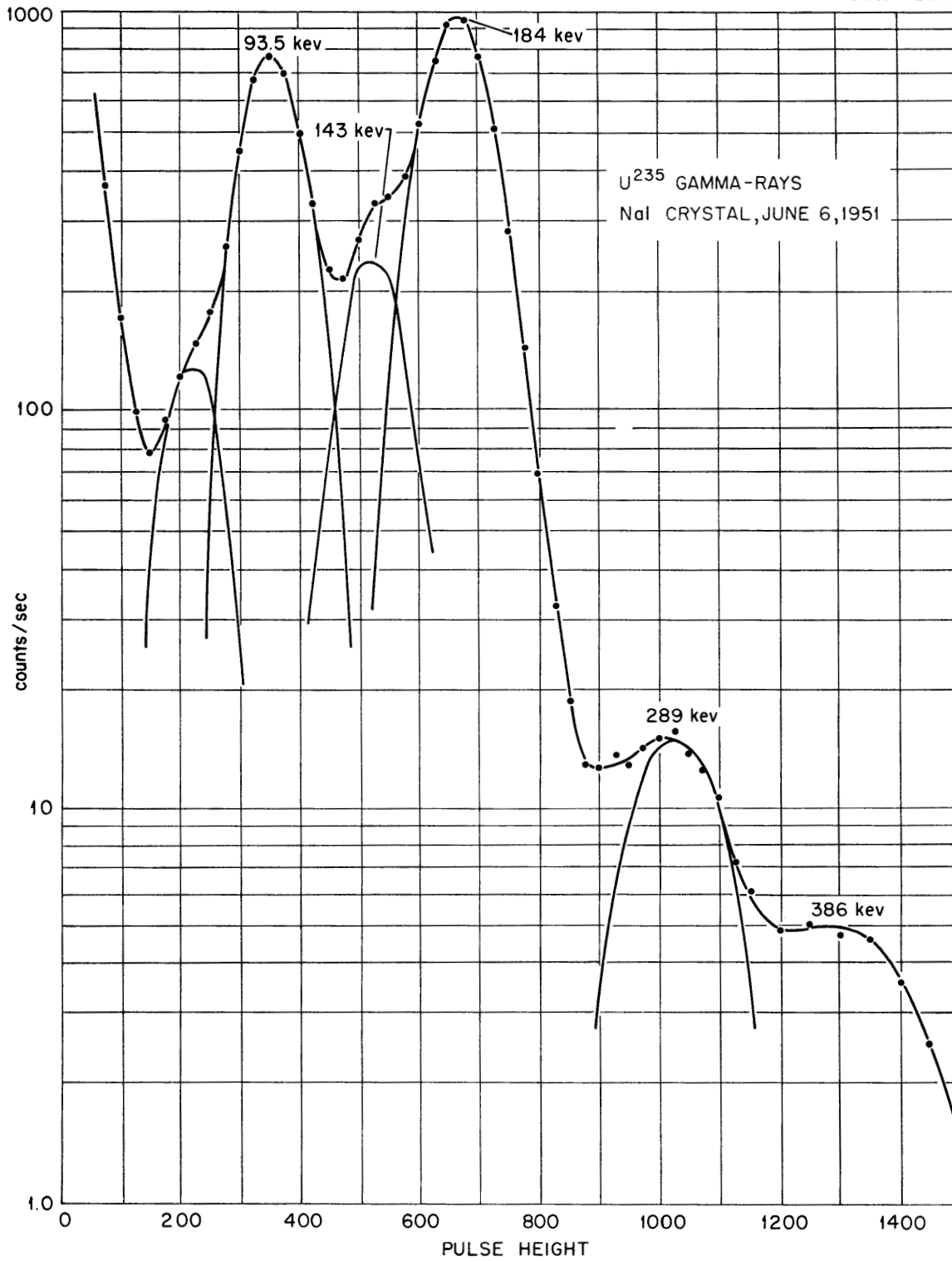


Fig. 1.1. Gamma-Ray Energy Spectrum of U^{235} .

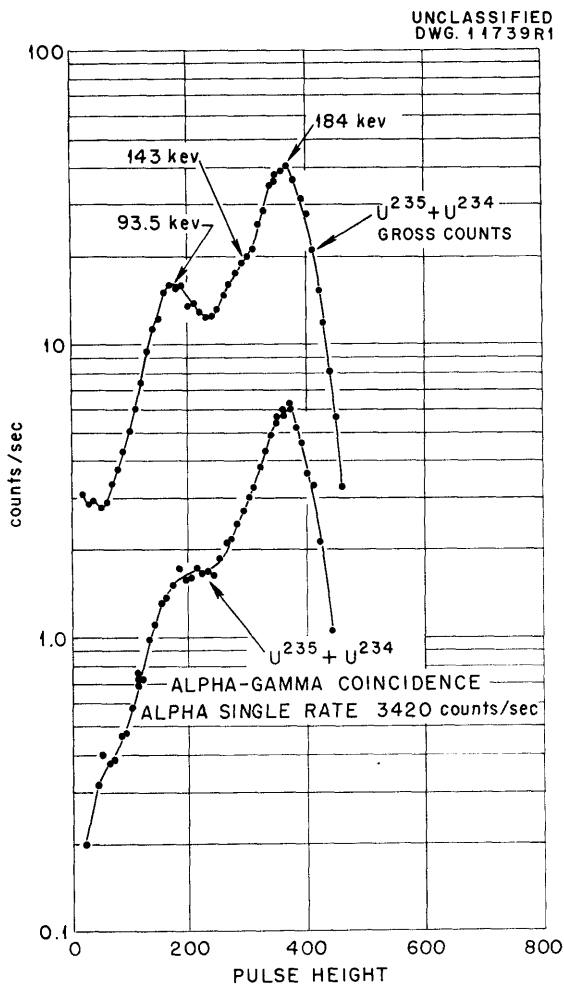


Fig. 1.2. Comparison Between the Gamma-Ray Energy Spectrum and Alpha-Gamma-Ray Coincidences for U^{235} and U^{234} .

energies and intensities of the other gamma rays are given in Table 1.1. It should be noted here that there was some self-absorption in both U^{235} and U^{234} samples due to their considerable thickness. In addition the intensity of the low-energy X ray is very much greater than is shown. When the X rays are absorbed in sodium iodide the condition of the

surface of the crystal is quite important since the X rays of low energy, such as the L X rays, are 90% absorbed in the first 0.005 in. of the surface and the amount of water vapor required to convert this 0.005 in. of surface into fluorescent inactive sodium iodide is very small. At this low an energy, intensity measurements with crystals are not reliable. An interesting feature of the U^{234} spectrum is the peak at 93 keV. Figure 1.4 shows the result measured with an earlier result on a sample of U^{234} that had been sitting undisturbed in a vault for some months. The upper curve was run first. After an interval of six days the second curve was run, and after a further interval of two months the curve in Fig. 1.3 was obtained. Between the time the first and second curves were run the sample had been transported, and the temperature of the container, which was not completely sealed, was changed during the transportation. Between runs for the second and third curves the sample was left undisturbed in the vault. The sample container was moderately tightly closed but not gas-tight sealed. The implication that the 93-keV peak results from an active gas is not yet certain, however, and further work is being done on these samples. The relative intensity of the 118- to 93-keV peak in the three measurements is 2.9, 4.8, 3.6.

Uranium²³⁶. The gamma-ray spectrum of a sample of U^{236} containing 95.13% U^{236} , 0.15% U^{234} and 4.18% U^{235} was measured and is shown in Fig. 1.5. Pure samples of U^{234} and of U^{235} were measured under the same conditions and in the same geometry. The U^{236} peaks at 93, 143, 184, 289, and 386 keV were found to be of the proper energy and intensity to be caused by the U^{235} content of the sample. When this contribution is subtracted from the total curve, the remainder has very nearly the same spectrum as U^{234} ,

PHYSICS DIVISION QUARTERLY PROGRESS REPORT

UNCLASSIFIED
DWG.11723R1

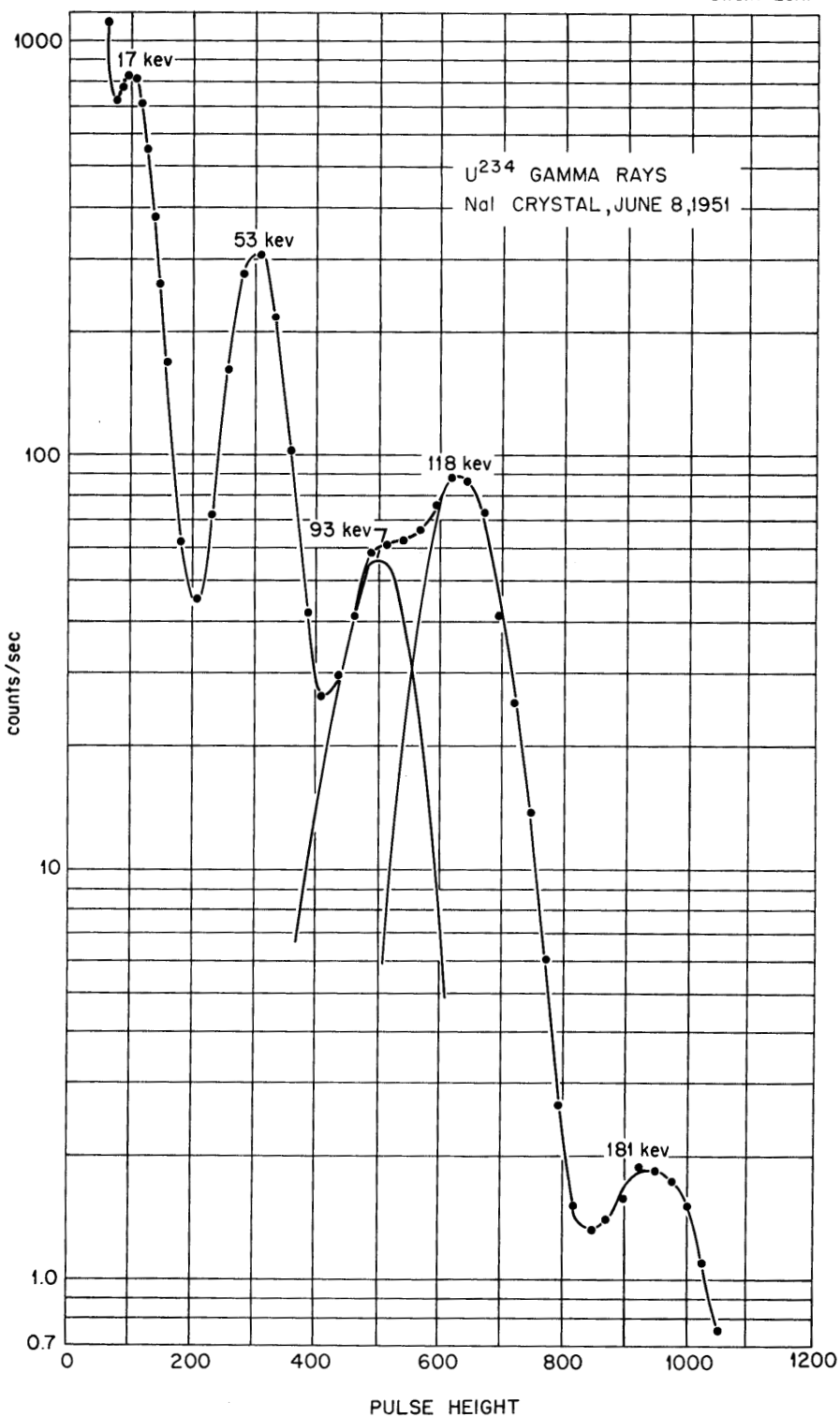


Fig. 1.3. Gamma-Ray Energy Spectrum of U^{234} .

FOR PERIOD ENDING SEPTEMBER 20, 1951

UNCLASSIFIED
DWG. 117 24R1

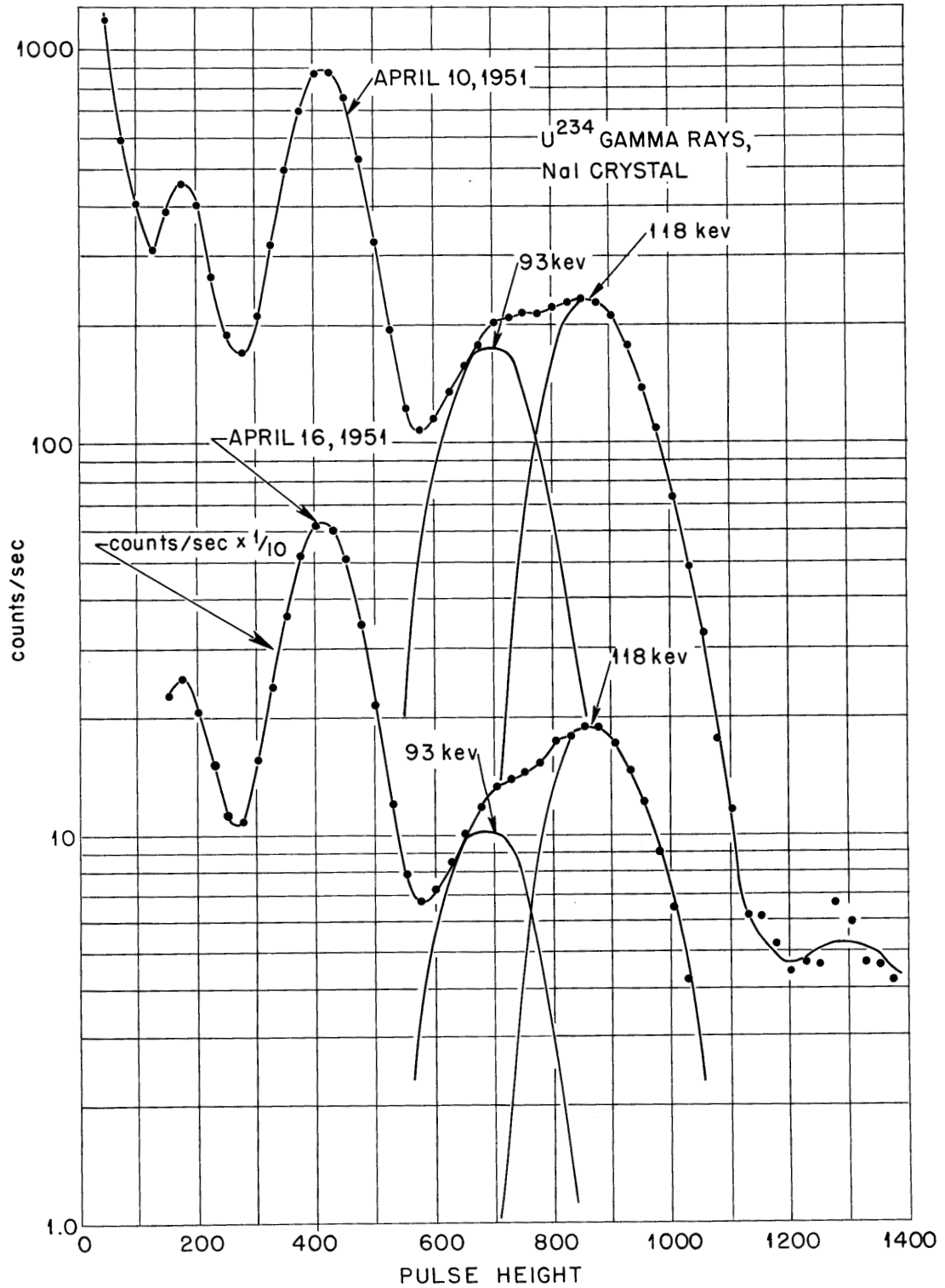


Fig. 1.4. Gamma-Ray Spectra for Same Sample of U²³⁴ as Determined Six Days Apart.

PHYSICS DIVISION QUARTERLY PROGRESS REPORT

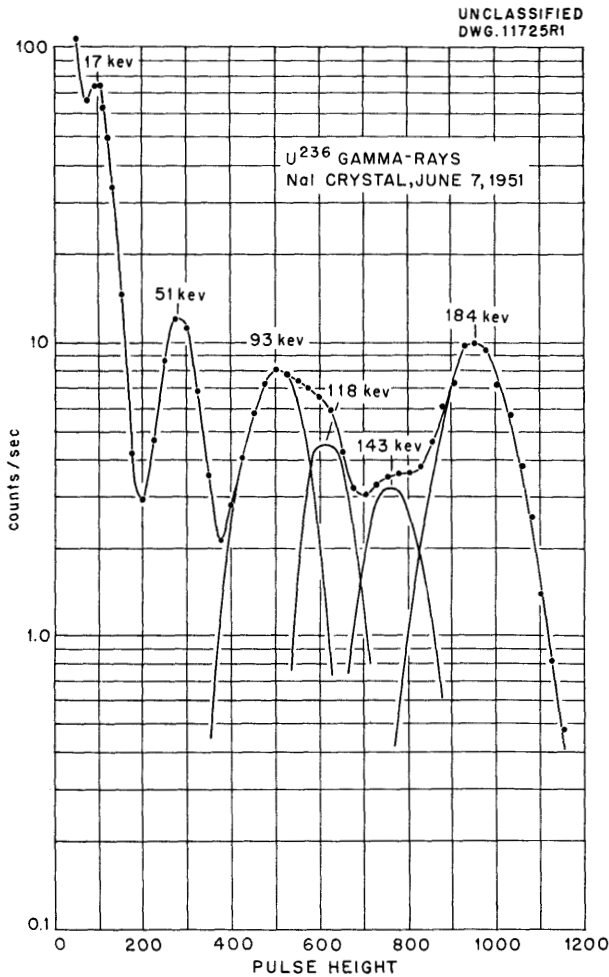


Fig. 1.5. Gamma-Ray Energy Spectrum Obtained for an Isotopically Impure Sample of U²³⁶.

except for the absence of the 93-kev peak, which appears with variable intensity in the U²³⁴ spectrum. However, the concentration of U²³⁴ in the U²³⁶ sample would have to be about five times greater than assayed to account for the intensity found.

TRANSITION-ENERGY DETERMINATION FOR ORBITAL CAPTURE

P. R. Bell M. Jauch
M. Cassidy

An element decaying by orbital electron capture to the ground state

of the daughter element has X rays of the daughter element as its principal detectable emission. There are, however, undetectable neutrinos and a weak but detectable gamma-ray continuum.⁽²⁾ This spectrum is analogous to the continuous gamma ray, generally called "internal bremsstrahlung," accompanying beta-ray transitions.^(3,4) The spectrum of the gamma rays accompanying beta transitions extends up to the maximum energy of the beta rays, and in the K-capture transitions the spectrum extends to the transition energy plus the energy obtained from the K electron captured by the nucleus. The energy from the K electron is the rest energy of an electron (0.511 Mev) less the K-orbit binding energy.

The shape of the gamma-ray spectrum to be expected from an allowed transition has been calculated by Morrison and Schiff,⁽¹⁾ and by Jauch,⁽⁵⁾ and is given by the relation

$$N(\omega)d\omega = C(\omega) \frac{d}{\pi m_0^2 c^4 W_0^2} \frac{\omega}{(W_0 - \omega)^2} d\omega, \quad (1)$$

where $N(\omega)$ is the number of photons lying in the energy interval $d\omega$ at energy ω . W_0 is the maximum photon energy which is related to the energy of transition E_0 by Eq. 2:

$$W_0 = E_0 + m_0 c^2 - E_k, \quad (2)$$

where $m_0 c^2$ is the self energy of an electron, and E is the K-shell binding

(2) P. Morrison and L. I. Schiff, "Radiative K Capture," *Phys. Rev.* 58, 24 (1940).

(3) C. S. Wu, "The Continuous X-Rays Excited by Beta Particles of ¹⁵P³²," *Phys. Rev.* 59, 481 (1941).

(4) J. K. Knipp and G. E. Uhlenbeck, "Emission of Gamma Radiation During the Beta Decay of Nuclei," *Physica* 3, 425 (1936).

(5) J. M. Jauch, to be published.

energy. The factor $C(\omega)$ is a complicated function that is slowly varying except at very low energies. The inner-bremsstrahlung spectrum is quite weak; the total number of photons goes as W_0^2 (4) and is about 3×10^{-5} per disintegration for Fe^{55} . The inner bremsstrahlung have been detected from Fe^{55} by Bradt *et al.*, (6) and their average energy has been estimated as 70 keV, yielding a transition energy of 150 keV.

A sample of Fe^{55} (containing a small amount of Fe^{59}) was measured with a scintillation spectrometer, (7,8) using a NaI-Tl phosphor. Figure 1.6 (upper curve) shows the pulse spectrum obtained. The lower curve is the pulse spectrum of a small sample of Fe^{59} . The low-energy end of the upper curve shows the continuous gamma-ray inner-bremsstrahlung spectrum. The strong peak at 190 ± 5 keV in both curves may be the missing crossover gamma ray of Fe^{59} not previously reported.* Other runs of these two samples were made at higher gain and the Fe^{59} contribution subtracted to obtain the Fe^{55} radiations. Such a spectrum is shown in Fig. 1.7.

An inspection of Eq. 1 shows its similarity to the relation for the beta-ray distribution given by the Fermi theory. If the experimental $N(\omega)$ is treated in the same way as it was for beta rays by Kurie, Richardson,

*Actually the low energy portion of the Fe^{59} spectrum appears to be quite complex, showing a number of gamma rays. Coincidence work is now in progress on this region of the spectrum.

(6) von H. Bradt, P. C. Gugelot, P. Huber, H. Medicus, P. Preiswerk, P. Scherrer and R. Steffen, "K-Einfang des Fe^{55} ," *Helv. Phys. Acta* 19, 222 (1946).

(7) P. R. Bell, "Pair Production and Photoelectric Effect in Scintillation Phosphors," *Science* 112, 7 (1950).

(8) P. R. Bell and J. M. Cassidy, "Measurement of the Gamma-Ray Energy of K^{40} ," *Phys. Rev.* 79, 173 (1950).

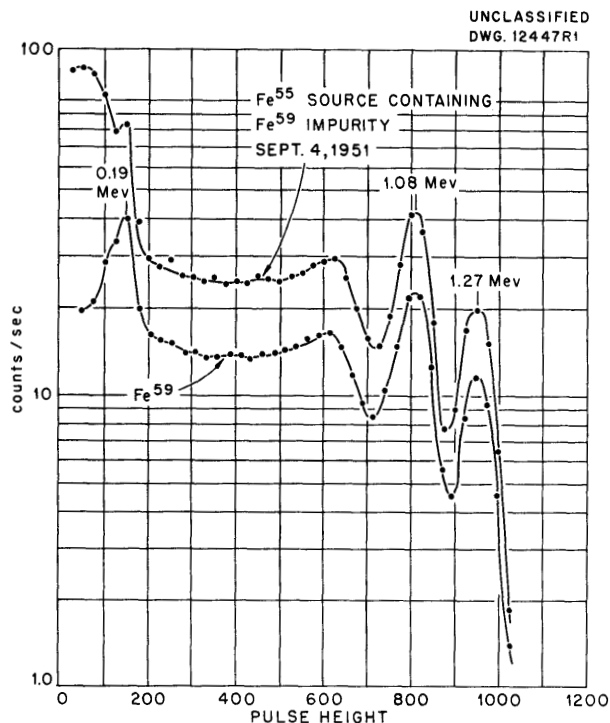


Fig. 1.6. Curves Showing Presence of Fe^{55} Inner-Bremsstrahlung Radiation in Mixture of Fe^{55} and Fe^{59} .

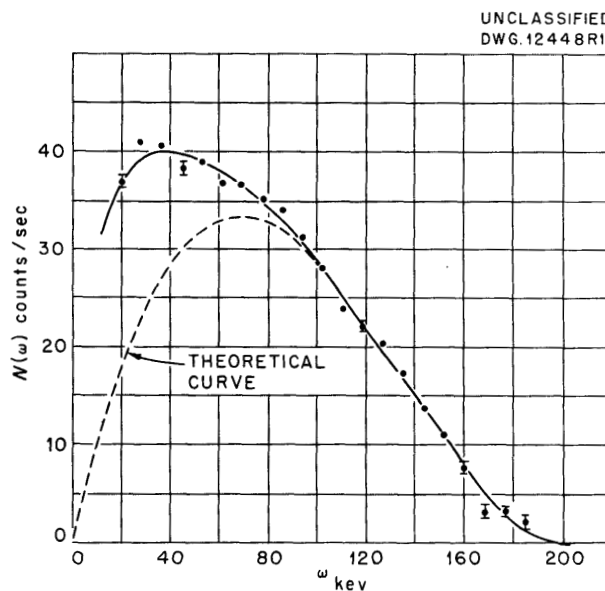


Fig. 1.7. Continuous Gamma-Ray Spectrum of Fe^{55} .

PHYSICS DIVISION QUARTERLY PROGRESS REPORT

UNCLASSIFIED
DWG. 12446R1

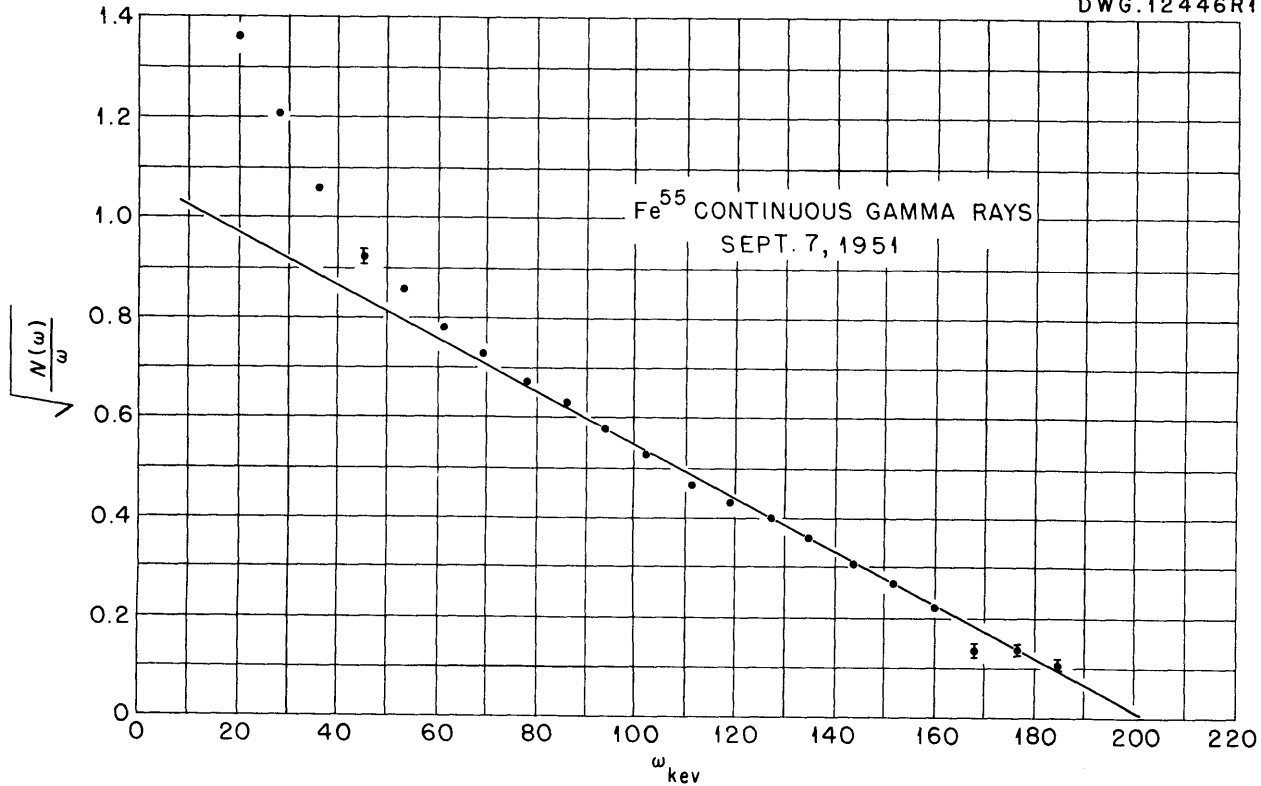


Fig. 1.8. End-Point Energy Determination for Gamma-Ray Continuum in Fe⁵⁵.

and Paxton,⁽⁹⁾ the following equation is obtained:

$$\frac{N(\omega)_{exp}}{C(\omega)} = K(W_0 - \omega), \quad (3)$$

where K is a constant. Since $C(\omega)$ is slowly varying, it may be considered constant to a first approximation.

Figure 1.8 shows the plot resulting from the data of Fig. 1.7. It is approximately linear, showing that the transition is allowed and intercepts the energy axis at $W_0 = 206 \pm 20$ kev.

This value for the transition energy including the K -electron energy must be considered approximate since correction has not been made for resolution and efficiency. Fortunately the efficiency of the crystal (2.5 cm thick) is very nearly unity for this energy range. The manganese X rays have been absorbed by the crystal container and a lucite absorber inserted to stop the Fe⁵⁹ electrons.

The energy of this transition can be obtained from the Q value for the Mn⁵⁵ (p, n) Fe⁵⁵ reaction. Using the value of $Q = 1.006$ Mev reported by Stelson and Preston⁽¹⁰⁾ the value

⁽⁹⁾F. N. D. Kurie, J. R. Richardson, and H. C. Paxton, "The Radiations Emitted from Artificially Produced Radioactive Substances," *Phys. Rev.* 49, 368 (1936).

⁽¹⁰⁾P. H. Stelson and W. M. Preston, "Fast Neutron Energies Determined by the Use of Resonant Scatters," *Phys. Rev.* 83, 469 (1951).

obtained is $W_0 = 217 \pm 10$ kev, which is in good agreement with the value obtained here.

This new method for K -capture transition energies is now being extended to other isotopes.

MEASUREMENT OF INTERNAL CONVERSION
COEFFICIENTS OF IODINE¹³¹

D. S. Hughes P. R. Bell
H. C. Thomas F. K. McGowan

The coincidence scintillation spectrometer has been used to measure the K -shell internal conversion coefficient (α^K) for the two cascaded gamma rays from I^{131} , namely, the 80- and 284-kev gamma rays. This was done by measuring the relative intensity of the xenon X ray and the given gamma ray in coincidence with the other member of the pair. Corrections for the efficiency of detection of the counters for the X rays and gamma rays were made. In the case of the 284-kev gamma ray it was necessary to estimate the number of gamma rays absorbed in the crystal and the fraction that produces pulses at the full gamma-ray energy (photo-peak). In the case of the 80-kev gamma ray most of the quanta passing through the crystal produce pulses at the photo-peak (some at the escape peak) so the correction factor is much less important. Measured values of the conversion coefficient are

$$\alpha^K(80 \text{ kev}) = 1.20 \pm 0.06 ,$$

$$\alpha^K(284 \text{ kev}) \approx 0.11 .$$

Rose, Goertzel, and Perry have published tables of relativistic values of conversion coefficients down to 150 kev. These can be extrapolated⁽¹¹⁾ to lower energies as

(11)P. Axel and R. F. Goodrich, *Internal Conversion Data*, NP-1921.

follows: the ratio of relativistic⁽¹²⁾ to nonrelativistic coefficients⁽¹³⁾ is plotted for $E_\gamma > 150$ kev and extrapolated to one at $E_\gamma = 0$; low-energy conversion coefficients are obtained by multiplying published tables of nonrelativistic coefficients by a correction factor from the ratio plot. Extrapolated values for $E_\gamma = 80$ kev, $z = 54$ are

$$\beta_1^K = 1.35 \text{ (magnetic dipole) ,}$$

$$\alpha_2^K = 2.51 \text{ (electric quadrupole) ,}$$

$$\alpha_1^K = 0.35 \text{ (electric dipole) .}$$

It thus appears that the 80-kev gamma ray is magnetic dipole. This assignment is supported by other data. The ground-state spin of Xe^{131} is $3/2$. Dipole radiation from the 80-kev excited state means a spin change of 1, hence the spin of the 80-kev state is either $1/2$ or $5/2$. Metzger has recently reported a spherically symmetric distribution of gamma rays that would be expected if the spin were $1/2$. R. E. Bell has observed that the 80-kev state is metastable with a half-life of 5×10^{-10} sec.

The agreement between measured and calculated conversion coefficients is not as good for the 284-kev gamma ray. Interpolated values from the tables of Rose, Goertzel, and Perry are as follows:

$$\beta_1 = 0.047 , \quad \alpha_2 = 0.041 ,$$

$$\beta_2 = 0.27 , \quad \alpha_3 = 0.16 .$$

(12)M. E. Rose, G. H. Goertzel, and C. L. Perry, *K-Shell Internal Conversion Coefficients; Revised Tables*, ORNL-1023 (June 25, 1951).

(13)M. H. Hebb and E. Nelson, "Internal Conversion of Gamma-Radiation in the L Shell," *Phys. Rev.* 58, 486 (1940).

PHYSICS DIVISION QUARTERLY PROGRESS REPORT

The measured value of $\alpha_k = 0.11$ does not agree well with any of the above values; one can only say that the radiation appears to be magnetic dipole, electric quadrupole, or electric octapole.

GAMMA RAYS FROM POTASSIUM⁴⁰

P. R. Bell M. Cassidy

Various phases of the study of gamma rays from K⁴⁰ have been under investigation for nearly two years and have been reported regularly in these quarterly reports. A separated sample of this isotope was recently obtained and used to obtain another measurement of the gamma-ray energy and an upper limit to the amount of positron radiation.

The scintillation spectrometer was used in conjunction with a 10-channel analyzer to measure the spectrum of the pulses produced when the NaI crystal was irradiated with K⁴⁰ gamma rays. The upper curve of Fig. 1.9 shows the spectrum in the neighborhood of the photoelectric peak. Calibration curves were run at the same gain setting using Co⁶⁰ and K⁴² as the gamma-ray source. (The curves were displaced downward in an arbitrary number of decades so there would be no interference.) Assuming a value of 1.332 Mev for the Co⁶⁰ gamma ray and a linear pulse-height scale results in a value of 1.462 Mev for the K⁴⁰ gamma ray. A similar procedure with K⁴² gamma rays for calibration (1.510 Mev) gives 1.460 Mev.

A further search has been made for the annihilation radiation that would

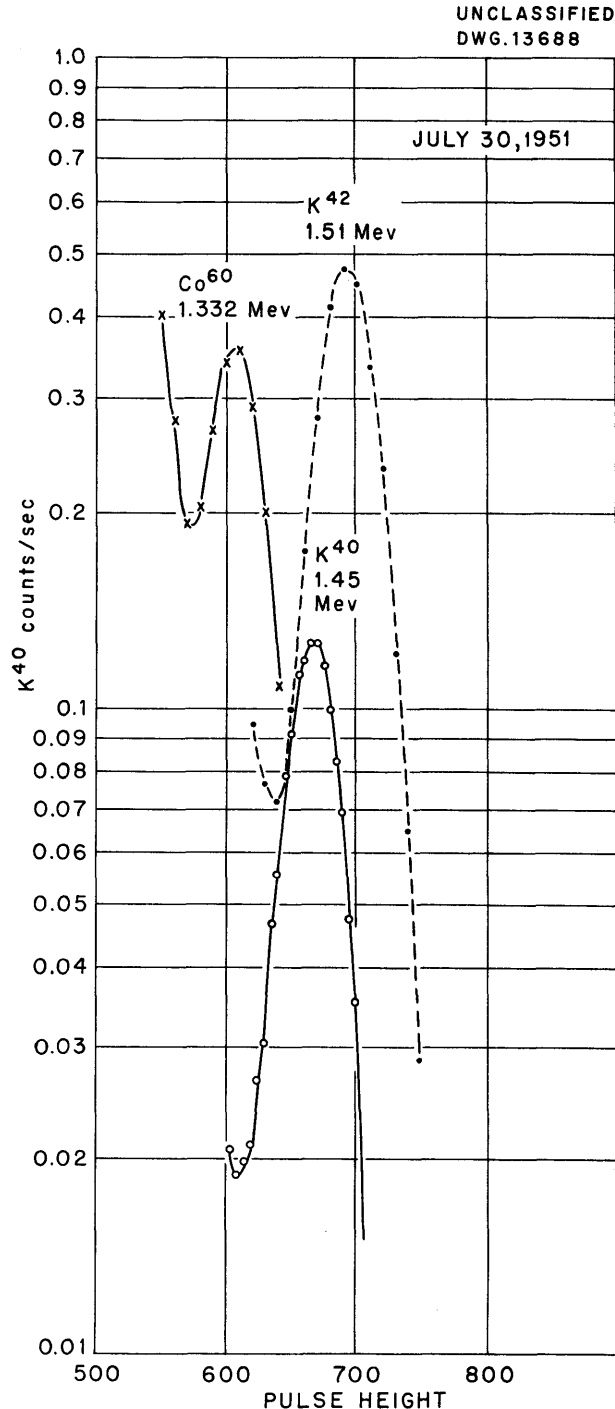


Fig. 1.9. Comparison Between K⁴⁰ Gamma-Ray Energy Spectrum and Calibration Spectra.

accompany positrons from the K^{40} . The pulse spectrum between 200 and 900 keV is shown in Fig. 1.10. The double row of points between 600 and 800 keV correspond to two sets of data taken at different times. Long counts were taken and several runs averaged in the region of 510 keV so that a small amount of annihilation radiation could be detected. The statistical error in this region is approximately the diameter of the circles. No evidence of such radiation can be seen in the curve of Fig. 1.10. In order to set an upper limit to the amount of such radiation that might exist and yet escape detection, a calculation was made of the number of positrons that would be required to boost the curve in the region of 510 keV by some 0.004 counts/sec, which is larger than the statistical error. (None of the points near 510 keV appears to depart from the smooth curve by such an amount.) From the known sensitivity of the crystal to annihilation radiation it was calculated that the number of positrons per beta disintegration must be less than 1/3600.

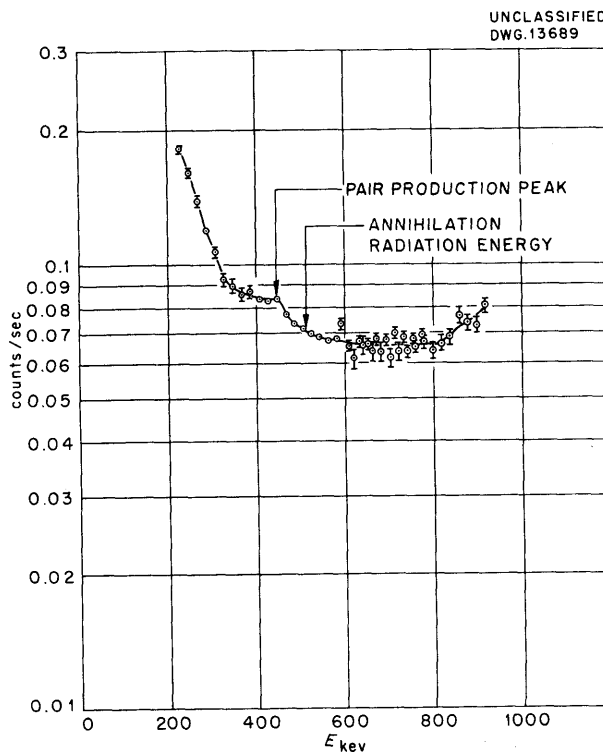


Fig. 1.10. Portion of Gamma-Ray Energy Spectrum of K^{40} Indicating an Upper Limit to the Amount of Annihilation Radiation Present.

PHYSICS DIVISION QUARTERLY PROGRESS REPORT

2. ELECTRONIC DEVELOPMENT

SINGLE-CHANNEL ANALYZER

J. E. Francis

Twelve of the analyzers reported previously (404A tubes in amplifier and discriminator) have been built by the Instrument Division and are in the process of being checked. Parasitic oscillations were encountered at some points and necessitated the addition of suppression resistors at strategic points. Modified circuit diagrams are now available. These analyzers show practically constant window width for all pulse heights when tested with a signal generator designed to produce pulses of shape similar to that obtained from the usual particle detectors. Many single-channel analyzers that work very well on square-top pulses show a big variation when tested in the foregoing manner.

MULTICHANNEL ANALYZERS

G. Kelley C. G. Goss
P. K. Bell

Two 10-channel analyzers have been in operation for several months and have proved very useful. Except for occasional scaler failures they have operated quite reliably. Nevertheless the research has been somewhat impeded by the limitation on integral counting rate. Circuit modifications have been made that decrease the resolving time from 10 to 7 μ sec. Even so the maximum counting rate that can be used is about 5000 counts/sec. The analyzer continues to operate at higher counting rates, but the spectrum becomes distorted. This defect is characteristic of most multichannel analyzers and results from using a gated amplifier. The window amplifier must be turned off during the time that a pulse is being analyzed. If a

pulse arrives during the interval of turning the amplifier back on, or if the tail of a pulse is present at this time, a count will be recorded in the wrong channel. Thus the counting rate must be kept low enough so that such a situation arises very infrequently.

The foregoing considerations have prompted the design of a new pulse-sorter chassis that operates on a different principle. When a pulse arrives at the window amplifier it is stored for 2.4 μ sec. If during this time no other pulses have arrived, the original pulse will be analyzed as it comes out of the delay line. This circuit is called an "inspector circuit." This scheme avoids the necessity of using a gated amplifier and hence does not encounter the difficulties described above.

The scheme for analyzing the pulse from the window amplifier is also changed considerably from the previous models. The pulse is lengthened and then analyzed by a group of long-tailed-pair discriminators. A simple anticoincidence circuit is used for determining the highest channel that was triggered by the pulse. The whole process is over in 2.6 μ sec and the analyzer is ready to receive the next pulse. This pulse sorter is faster and more reliable than the one used previously; in addition the circuit is considerably simplified, so much so that it is now planned to construct a 20-channel analyzer to fit into a 6-ft relay rack.

DISCRIMINATOR-TUBE DRIFTS

G. G. Kelley C. G. Goss

Analyzers of the type described in the previous section require

discriminators that do not drift appreciably. Tests have been made to determine which tubes are most suitable in this respect. A long-tailed-pair arrangement was used, with the grids being held at fixed potentials that were chosen equal to the grid potentials actually obtaining in a discriminator at the instant of firing. The difference in the plate currents was recorded on a strip chart. Tests on various pairs of tubes were run over a period of six weeks. The data shown in Table 2.1 were taken from these strip charts.

SCALER IMPROVEMENTS

P. R. Bell C. G. Goss
G. G. Kelley

The scaler in the multichannel analyzers use 12AT7 tubes and fail by "scaling through" as the tubes age. This type of failure is characteristic of Higinbotham scalers when tubes are used that have a short grid base, i.e., tubes which are cut off with only a small negative grid voltage. Consider the following situation in a group of three scaling

TABLE 2.1

Plate-Current Excursions

RUN NO.	TUBE TYPE	AVERAGE DAILY EXCURSION (mv)	AVERAGE WEEKLY EXCURSION (mv)
1	12AT7	12	17
2	12AT7	6.6	18
3	6AU6	8.1	15
4	6AU6	5.6	9.2
5	6AK5	6.5	22
6	5654	10.9	31

The maximum deviation in plate current was determined for each day and for each week. This figure was converted to equivalent change in potential of one of the grids of the pair. Column 3 is the average of the daily excursions expressed in millivolts of grid change. Column 4 is the average of the weekly excursions. It appears that the 12AT7 and 6AU6 tubes are somewhat better than the 6AK5 or 5654 tubes. Even the 5654-tube drift of about 30 mv/week would amount to only a 1% change in the "window width" of the analyzer.

stages: the first scale in the 0 position, the second scale in the 0 position, and the third scale in the 1 position. As the first scale flips to the 1 position, the third scale may be flipped. This undesirable situation is caused by the release of diode current from the plate of the "off" tube of the second scale producing a small positive surge at the grid of the "on" tube of this scale and a corresponding negative pulse at its plate. Since this plate bears the coupling diodes and is already down, one of the diodes is

3. SHORT-LIVED ISOMERS AND DIRECTIONAL ANGULAR CORRELATION OF SUCCESSIVE GAMMA RAYS

F. K. McGowan

E. D. Klema

In a recent paper⁽¹⁾ on the classification of nuclear isomers, Goldhaber and Sunyar have classified the isomer Re^{187} (5.5×10^{-7} sec) as an $M2$ (magnetic quadrupole) transition on the basis of the lifetime agreeing fairly well with Weisskopf's one-particle formula for magnetic transitions. Also the K/L conversion ratio of five⁽²⁾ lends strong support for the magnetic character of the 133-keV gamma-ray transition with $Z = 75$. To check the multipole order assignment, the K -shell conversion coefficient has been measured using a NaI scintillation spectrometer. Under favorable circumstances the measured intensity ratio of the K X ray to the gamma ray is a measure of the K -shell conversion coefficient α^K provided the appropriate corrections for fluorescent yield, detection efficiency, and escape-peak intensity are made. The α^K obtained from the "single count" gamma-ray spectrum for the 133-keV transition is ≤ 3.2 . The upper limit is indicated because internal conversion of higher energy gamma rays from $\text{W}^{187} \rightarrow \text{Re}^{187}$ will contribute to the observed K X-ray intensity. A coincidence measurement of the intensities will give α^K directly, and this is being done. In the meantime it is of interest to compare the measured upper limit of α^K with the theoretical K -shell conversion coefficients.⁽³⁾ These are $\alpha_2^K = 0.48$,

$\alpha_3^K = 1.30$, $\beta_1^K = 2.40$, and $\beta_2^K = 13.0$. The measured upper limit indicates that the $M2$ assignment is incorrect for the 133-keV transition. This may thus be a transition ($M1 + E2$) with the $M1$ character being predominant.

The 6.7-day Lu^{177} β^- activity is known to decay by three beta groups to Hf^{177} .⁽⁴⁾ The lowest energy beta group leads to an excited state in Hf^{177} followed by two gamma rays in cascade with energies of 206 and 112 keV. The half life of the excited state 112 keV above the ground state is $T_{1/2} < 5 \times 10^{-10}$ sec as measured with the delayed coincidence scintillation spectrometer using anthracene detectors. The gamma-ray spectrum has been examined with a NaI scintillation spectrometer. Figure 3.1 is the spectrum taken at sufficiently low geometry in order that the 318-keV crossover transition peak is due to the 318-keV gamma ray alone and not a coincidence pulse due to the 206- and 112-keV gamma rays. At high geometry an additional peak is also obtained in the spectrum at 261 keV which is the coincidence pulse from the 206-keV gamma ray plus the 55-keV X ray. The peaks have been resolved into Gaussian components and the intensity of the crossover transition from the 111-keV excited state is measured to be between 4 and 5%.

Since the lifetime of the intermediate state at 112 keV is sufficiently small, the 206- and 112-keV gamma-ray cascade appeared to be an ideal case in which to investigate the directional angular correlation

(1) M. Goldhaber and A. W. Sunyar, "Classification of Nuclear Isomers," *Phys. Rev.* 83, 906 (1951).

(2) F. K. McGowan, *Short-Lived Isomeric States of Nuclei*, ORNL-952, p. 104 (March 13, 1951).

(3) M. E. Rose, G. H. Goertzel, and C. L. Perry, *K-Shell Internal Conversion Coefficients; Revised Tables*, ORNL-1023 (June 25, 1951).

(4) D. G. Douglas, "Radiations from Lu^{177} ," *Phys. Rev.* 75, 1960 (1949).

PHYSICS DIVISION QUARTERLY PROGRESS REPORT

UNCLASSIFIED
DWG. 13691

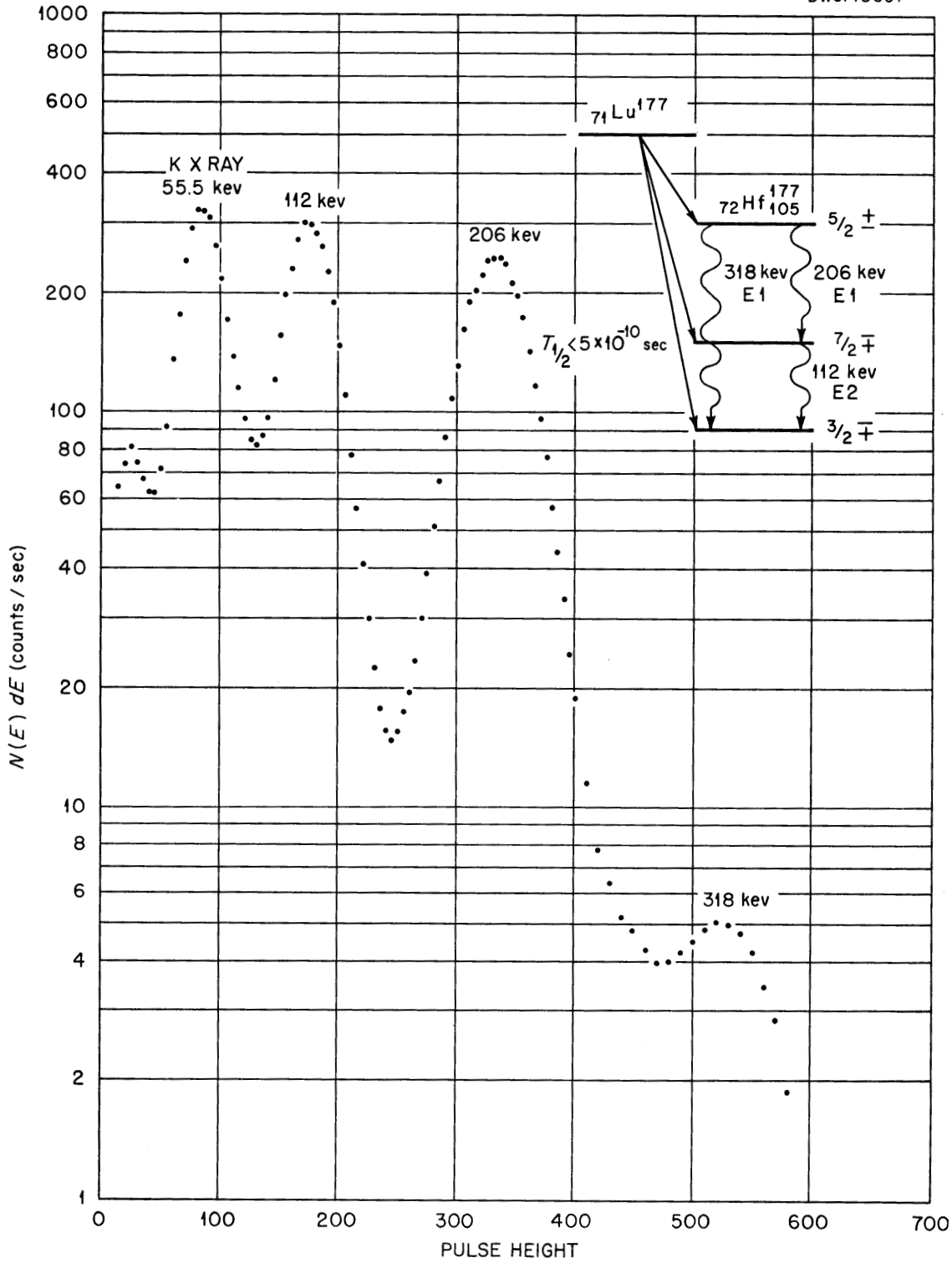


Fig. 3.1. Gamma-Ray Spectrum from Hf^{177} .

of successive gamma rays. The angular correlation has been examined with a coincidence scintillation spectrometer using NaI detectors and is found to be anisotropic. The gamma rays entering into the angular correlation measurement are selected according to their energy. In this case one detector selects the 206-keV gamma ray and the other detector the 112-keV gamma ray. The coincidence resolving time is 10^{-7} sec and the angular resolution is ± 12.7 degrees. The latter was determined by observing the coincidence rate due to annihilation quanta from a Na^{22} source as a function of angle. These quanta are known to be practically collinear. Under these conditions, for the case of the gamma rays in Hf^{177} , the true coincidence rate is of the order of 2.5 counts/sec, whereas the random rate is 8% of the true rate. Figure 3.2 shows the observed angular distribution. The ordinate represents

$$\epsilon(\theta) = \frac{n(\theta) - n(\pi/2)}{n(\pi/2)} = W(\theta) - 1,$$

where

$$W(\theta) = 1 + \sum_1^n a_{2i} \cos^{2i}\theta.$$

The solid curve represents $\epsilon(\theta) = -0.213 \langle \cos^2\theta \rangle$, where $\langle \cos^2\theta \rangle$ has been averaged over the finite angular resolution of the apparatus. $W(\theta) = 1 - 0.213 \cos^2\theta$ is characteristic of a successive dipole \rightarrow quadrupole transition, with angular momenta $5/2 \rightarrow 7/2 \rightarrow 3/2$ for the three states in order of decreasing excitation energy. The measured contribution of the 318-keV transition by a Compton scattering between the two detectors is 0.01% of the true coincidence rate.

In order to determine the character of the transitions and relative parity of the states the K -shell

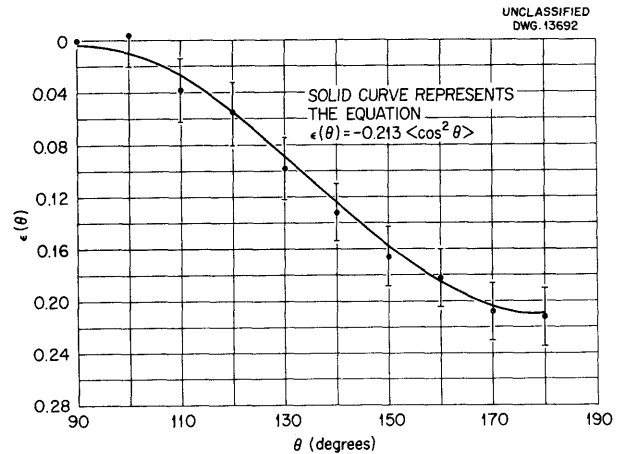


Fig. 3.2. Angular Distribution of the Coincident Gamma Rays from Hf^{177}

internal conversion coefficients have been measured. The measurement of α^K consists essentially in measuring the intensity ratio of the K X ray to the gamma ray in coincidence with the other gamma ray of the cascade by means of a coincidence scintillation spectrometer employing NaI detectors. There are several corrections to be applied to the experimental observations, and these along with the results for α^K are tabulated in Table 3.1.

The result for α^K (206 keV) is tentative because there are some experimental difficulties connected with the measurement. Lead X rays interfere when a lead diaphragm is used between the two detectors to suppress the effect of Compton scattered gamma rays from one detector to the other. In the case of α^K (112 keV) no diaphragm was necessary for the measurement because the energies of Compton scattered gamma rays do not interfere in any way with the peak intensities measured. In Table 3.2 the various theoretical conversion coefficients are listed along with α_{exp}^K .

PHYSICS DIVISION QUARTERLY PROGRESS REPORT

TABLE 3.1

Experimental Results from Lu¹⁷⁷

E_γ (keV)	INTENSITY RATIO (uncorrected)	FLUORESCENT YIELD ω_K	INTENSITY OF ESCAPE PEAK	$\frac{\omega_\gamma^*}{\omega_x}$	FRACTION OF DETECTED γ RAYS IN FULL ENERGY PEAK	α^K
112	0.69	0.937	15%	0.95	1.0	0.82 ± 0.08
206	0.11	0.937	15%	0.80	0.92	≤ 0.10

* ω_γ/ω_x is a correction for the effective solid angle that the NaI detector subtends to the source. At close distances (~ 1 cm) the effective geometry is very energy dependent for gamma radiation. This was pointed out by P. R. Bell.

TABLE 3.2

Comparison of Theoretical Conversion Coefficients with the Experimental Coefficients

E_γ (keV)	α_1^K	α_2^K	β_1^K	α_{exp}^K
112	0.22	0.80	2.8	0.82 ± 0.08
206	0.045	0.153	0.52	≤ 0.10

The agreement between α_2^K and α_{exp}^K for the 112-keV transition is quite good, and it is concluded that the transition is of the E2 (electric quadrupole) type. Although the measurement of α^K (206 keV) is incomplete, the tentative result definitely excludes an M1 transition. The uncertainties in the measurement appear to be such as to reduce α_{exp}^K , which would favor an E1 assignment. This multipole order is compatible with the conclusion obtained from the angular correlation. On the other hand if one forces the 206 transition to be of the E2 type, there are no favorable quadrupole \rightarrow quadrupole combinations (by favorable is meant that the gamma rays are emitted with the lowest angular momentum allowed by angular momentum selection rules) compatible with the observed magnitude

($a_2 = -0.21 \pm 0.02$) of the anisotropy. The unfavorable quadrupole \rightarrow quadrupole combinations and the other dipole \rightarrow quadrupole combinations with the correct magnitude for the anisotropy may be excluded conclusively, either on the basis of the observed shape of the angular correlation distribution or the fact that the ground state is restricted to $j \leq 3/2$.⁽⁵⁾ It appears that both the internal conversion data and the angular correlation are consistent with the interpretation that both transitions are pure multipoles.

In Fig. 3.1 a proposed level scheme for Hf¹⁷⁷ is shown on the basis that the 206- and 112-keV gamma rays are E1 and E2 transitions, respectively. Mayer's shell model would predict either a $p_{3/2}$ or $f_{5/2}$ orbit for Hf¹⁷⁷ with $N = 105$. Although relative parities are indicated in Fig. 3.1, the shell model predicts the ground state to be odd parity, and the parities of the excited states would be odd and even in the order of increasing energy. The crossover transition of 318 keV is of the E1 type and should compete favorably

(5) E. Rasmussen, "Hyperfeinstruktur im Hafniumspektrum," *Naturwiss.* 23, 69 (1935).

FOR PERIOD ENDING SEPTEMBER 20, 1951

with the 206-kev transition. The transition probability--energy relations as derived by Dancoff or Weisskopf predict the relative intensity of the 318-kev transition to the 206-kev transition to be four. The observed intensity ratio is 80 times smaller. This indicates that

for transitions between states in a given nucleus the "scatter" of the square of the matrix element is very large. Thus one should use the theoretical estimates for transition probabilities with extreme caution in estimating intensities of crossover transitions.

PHYSICS DIVISION QUARTERLY PROGRESS REPORT

4. SHORT-PERIOD ACTIVITIES

E. C. Campbell J. H. Kahn*
K. L. Robertson

LEAD ISOMER OF 0.9-sec HALF LIFE

E. C. Campbell

It was previously reported⁽¹⁾ that when pure lead is irradiated with pile neutrons, an activity having a half life of 0.9 sec is produced. Measurements of the radiations associated with this activity by means of a NaI scintillation spectrometer with photographic recording show two gamma rays of about equal intensity having energies of 0.55 ± 0.02 and 1.05 ± 0.02 Mev. Samples enriched in each one of the naturally occurring isotopes of lead were irradiated, and only in samples enriched in Pb^{207} was a significant amount of the activity found.

In order to find out whether thermal neutrons are responsible for producing the activity, samples of lead were irradiated in a separable rabbit, one part of which was made of cadmium. The cadmium was in the form of a hollow box about 1/8 in. thick surrounding the sample on all but one side. This form was necessary to permit automatic stripping of the box to avoid cadmium activity when the sample was brought to rest in front of the NaI scintillation counter. Comparison was made of the 0.9-sec activity produced in this way with the activity produced when the same sample was irradiated in a similar box made of magnesium. It was found that cadmium reduced the initial activity of the lead to about 80% of what it was without the cadmium.

*ORINS, Graduate Fellow University of Tennessee.

(1) E. C. Campbell and M. Goodrich, "Scintillation Spectra of Short-Life Activities," *Phys. Rev.* 78, 640 (1950).

Under the same conditions the 54-min activity of indium was reduced by the cadmium cover by a factor of 5.2. It appears, therefore, that the lead activity is not due to absorption of thermal neutrons.

This result still does not permit the activity to be assigned unambiguously. It does exclude the (n,γ) reaction, since this reaction would be expected to be produced by thermal neutrons. Of the possible fast-neutron reactions, the (n,p) and (n,α) appear to be excluded due to the high potential barrier for the outgoing particle. The $(n,2n)$ reaction is possible but seems unlikely on energetic grounds. More likely is the (n,n^*) reaction (inelastic scattering) which is, for example, the process known to be responsible for the production of the 7.4-sec Au^{197m} from stable Au^{197} by fast neutrons.⁽²⁾ If this interpretation is correct, the activity is assignable to a metastable state of Pb^{207} .

Evidence on the excited levels in Pb^{207} has been obtained from the study of the K -capture decay of Bi^{207} and the alpha decay of 0.52-sec⁽³⁾ Po^{211} by Neumann and Perlman.⁽⁴⁾ They deduce the existence of levels at 0.54 ± 0.04 and at 1.063 ± 0.005 Mev, as well as many more. The agreement within experimental error of these values with the energies of

(2) A. A. Ebel and C. Goodman, "Metastable States in In^{115} and Au^{197} ," *Phys. Rev.* 82, 130 (1951).

(3) R. F. Leininger, E. Segrè, and F. N. Spiess, "The Half-Life of $Ac-C'$," *Phys. Rev.* 82, 334 (1951).

(4) H. M. Neumann and I. Perlman, "Long-Lived Bi^{207} and Energy Levels of Pb^{207} ," *Phys. Rev.* 81, 958 (1951).

the gamma rays from the 0.9-sec activity may be fortuitous; if the identification is accepted, however, then the gamma rays emitted following the emission of the short-range alpha particle (6.34 Mev) from Po^{211} should show the 0.9-sec half life. This point may be subject to experimental check. From measurements on the proton ranges from the (d,p) reaction on Pb^{206} , Harvey⁽⁵⁾ deduces levels of Pb^{207} at 0.62 ± 0.10 and 0.95 ± 0.10 Mev, in addition to other levels. The agreement is not so convincing although still within experimental error.

On the basis of the general systematics of nuclear isomers and the shell model, Goldhaber and Sunyar⁽⁶⁾ have assigned the 0.9-sec activity to an $M4$ transition (1.05 Mev) followed by an $E2$ transition (0.5 Mev). The level assignments are $i_{13/2} \rightarrow f_{5/2} \rightarrow p_{1/2}$. This implies that the isomeric level is 1.5 Mev above the ground state. This assignment is not in disagreement with any of the evidence cited since it may be argued that transitions through this high-spin level following alpha- or electron-capture decay may be strongly forbidden by selection rules. The authors state in a footnote that an unpublished analysis of the Pb^{207} levels by M. H. L. Pryce lends further support to their assignment.

ERBIUM ISOMER (2.5 sec)

E. C. Campbell J. H. Kahn
M. Goodrich*

The discrepancy previously pointed out⁽⁷⁾ between the K conversion

coefficient and the multipole order required by the lifetime-energy relationship of the 210-keV transition in the 2.5-sec isomer of erbium has been resolved. Goldhaber and Sunyar,⁽⁶⁾ on the basis of a revised lifetime-energy relationship, have assigned the transition to the electric 2^3 pole ($E3$) classification instead of 2^4 pole. The value of the K conversion coefficient deduced from our measurements of the ratio of K X rays to gamma rays was between 0.05 and 0.10. This value was appropriate to an $E1$ or $E2$ transition, either of which would have a much shorter half life than that observed.

Upon re-examination of the experimental setup in a search for systematic errors, it was found that the conical collimator between the extended source and NaI crystal allowed a greater fraction of gamma rays to be detected than of X rays. Substitution of no collimation or of good collimation (a 1/4-in. hole through 1.5 in. of lead) gave substantially the same result, namely, that the ratio of the area of the X-ray peak to that of the gamma-ray was 0.50. From this is deduced (after making small corrections for fluorescent yield and for the relative efficiencies of the crystal for the two radiations) a K conversion coefficient of 0.55 ± 0.1 , which is in satisfactory agreement with that computed by Rose, Goertzel, and Perry⁽⁸⁾ for an $E3$ transition, namely, 0.49. In addition the K -to- L ratio experimentally found is in good agreement with the semiempirical curve of Goldhaber and Sunyar.

*Consultant, Louisiana State University.

(5) J. A. Harvey, *M.I.T. Laboratory for Nuclear Science and Engineering (Sixteenth) Progress Report: (First Quarter of 1950)*, NP-1586 (April 1, 1950).

(6) M. Goldhaber and A. W. Sunyar, "Classification of Nuclear Isomers," *Phys. Rev.* 83, 906 (1951).

(7) E. C. Campbell, "Short Period Activities," *Physics Division Quarterly Progress Report for Period Ending December 20, 1950*, ORNL-940, p. 16 (March 15, 1951).

(8) M. E. Rose, G. H. Goertzel, and C. L. Perry, *K-Shell Internal Conversion Coefficients; Revised Tables*, ORNL-1023 (June 25, 1951).

PHYSICS DIVISION QUARTERLY PROGRESS REPORT

PROPORTIONAL COUNTER SPECTROMETER

J. H. Kahn

During the past quarter a terminal report (Ph.D.Dissertation) by J. H.

Kahn entitled "An Investigation of X-ray and Gamma-ray Spectra of Short Period Radioisotopes" has been issued as ORNL-1089.

5. HIGH-VOLTAGE ACCELERATOR PROGRAM

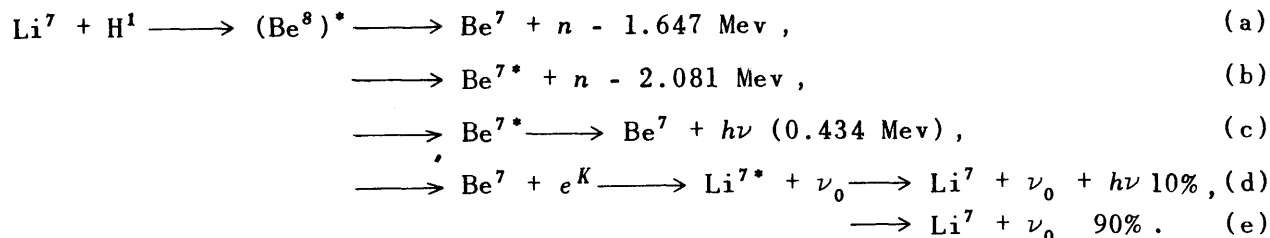
NEUTRON CROSS SECTIONS

Preliminary to putting the 6-Mev Van de Graaff generator into service as a neutron generator, several studies have been made extending to higher energy the neutron yield vs. energy of a number of (p,n) reactions. Neutron yields need to be known not only for determining possible neutron sources, but also to determine what materials can be used for slits, collimator tubes, etc., with minimum background. In addition, it is necessary to be able to recognize what effects common impurities can give. The following is a summary of several (p,n) yields obtained to date.

 $\text{Li}^7(p,n)\text{Be}^7$ REACTION

H. B. Willard T. M. Hahn
J. K. Bair J. D. Kington

Neutrons are produced when lithium is bombarded with protons; the following reactions take place:



The primary neutron group (a) has a measured threshold of 1.882 Mev for neutrons emitted in the forward direction.⁽¹⁾ The secondary neutron group (b) arises from an excited state,⁽²⁾ 434 keV above the ground

(1) R. G. Herb, S. C. Snowdon, and O. Sala, "Absolute Voltage Determination of Three Nuclear Reactions," *Phys. Rev.* 75, 246 (1949).

(2) H. B. Willard and W. M. Preston, "The First Excited State of Be^7 from the $\text{Li}^7(p,n)\text{Be}^7$ Reaction," *Phys. Rev.* 81, 480 (1951).

state in Be^7 , and therefore has a threshold of 2.374 Mev. Group (b) is not more than 10% of the primary group below 4 Mev. The total yield of neutrons from this reaction has been measured up to 4.2 Mev by several laboratories.^(3,4,5) In this energy range, the yield exhibits the well-known "geometric peak" just above threshold and a resonance for the formation of the compound nucleus $(\text{Be}^8)^*$ at 2.3 Mev. The yield is flat from 2.8 to 4.2 Mev.

In this experiment the yield was extended to above 5 Mev. A thin metallic layer of lithium was evaporated on the tantalum cup of a rotating target. The neutrons were detected with a long counter placed 1 meter from the target in the forward direction. The resultant curve of neutrons detected per unit charge of proton current (measured with a conventional beam-current integrator) is plotted in Fig. 5.1 as a function of proton energy. The yield shows the

geometric peak which indicates a target thickness of less than 11 keV (at threshold), the resonance in the compound nucleus at 2.31 Mev, and a

(3) J. E. Hill and W. E. Shoupp, "Excitation Function for Proton-Neutron Reaction in Lithium ($\text{Li}^7(p,n)$)," *Phys. Rev.* 73, 931 (1948).

(4) R. Taschek and A. Hemmendinger, "Reaction Constants for $\text{Li}^7(p,n)\text{Be}^7$," *Phys. Rev.* 74, 373 (1948).

(5) H. B. Willard, M.I.T. Ph.D. Thesis (1950).

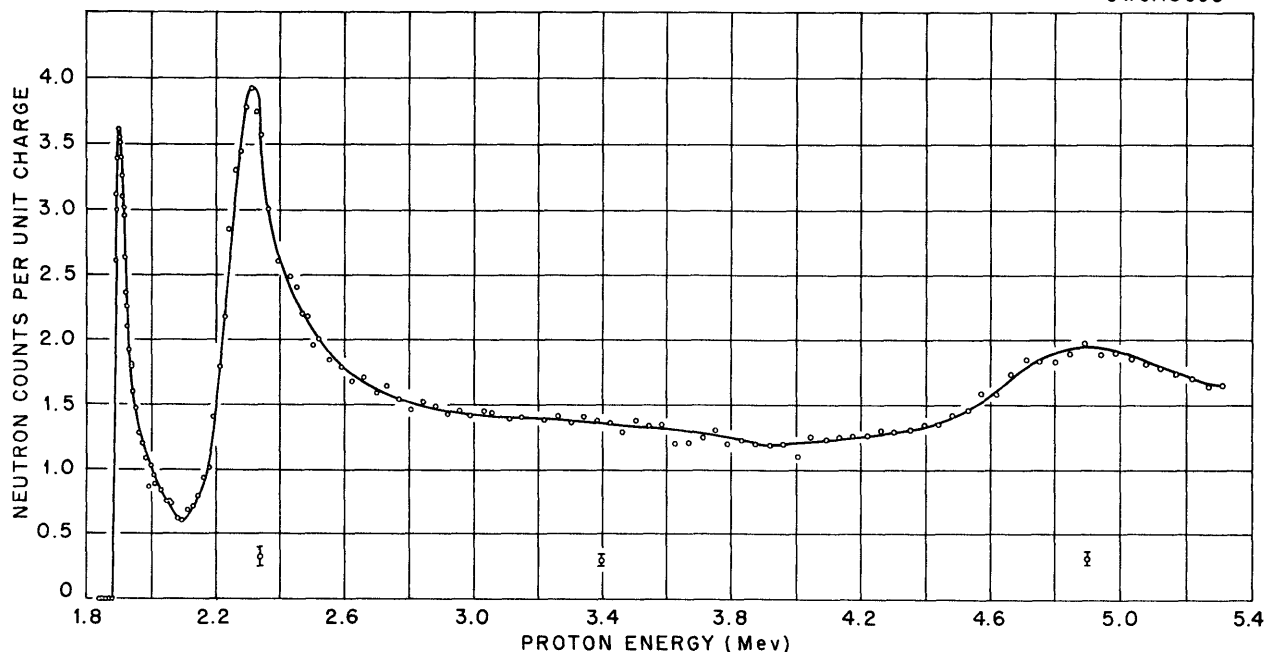


Fig. 5.1. $\text{Li}^7(p,n)\text{Be}^7$ Yield (in the Forward Direction).

new level whose maximum comes at an energy of 4.90 Mev. The full width of this new level at half maximum is about 0.6 Mev.

The measurement of (p,n) thresholds and the detection of inelastically scattered neutrons is facilitated by a counter that has its highest sensitivity for low-energy neutrons. Such a device has been described by Bonner and Butler.⁽⁶⁾ This "Bonner-type" counter consists of a BF_3 counter surrounded by a paraffin cone of half-angle 27 deg (with numerous axial holes drilled through it). The response of this counter has been measured by placing it at +20 deg and a long counter at -20 deg with respect to the proton beam, using the $\text{Li}^7(p,n)\text{Be}^7$ reactions as a source. Both counters were located at the proper distances

from the target to subtend approximately the same solid angle. A plot of the ratio of counts in the Bonner counter to counts in the long counter, Fig. 5.2, is essentially the energy sensitivity curve for the Bonner counter, since the long counter has a relatively flat response to neutrons in the energy range considered here. This curve shows that the Bonner counter offers good discrimination for neutrons below 100 kev.

$\text{Be}^9(p,n)\text{B}^9$ REACTION

J. K. Bair T. M. Hahn
H. B. Willard C. W. Snyder

The neutron yield from protons on beryllium has been repeated with the improved resolution and absolute energy determination available. The curve shown in Fig. 5.3 indicates by the geometric peak a target thickness of 6 kev. The known level in B^{10} appears at 2.57 Mev, and a new level

(6) T. W. Bonner and J. W. Butler, "Neutron Thresholds from the Reactions $\text{T}^3(p,n)\text{He}^3$, $\text{Li}^7(p,n)\text{Be}^7$, $\text{Be}^9(d,n)\text{B}^{10}$, and $\text{O}^{16}(d,n)\text{F}^{17}$," *Phys. Rev.* 83, 1091 (1951).

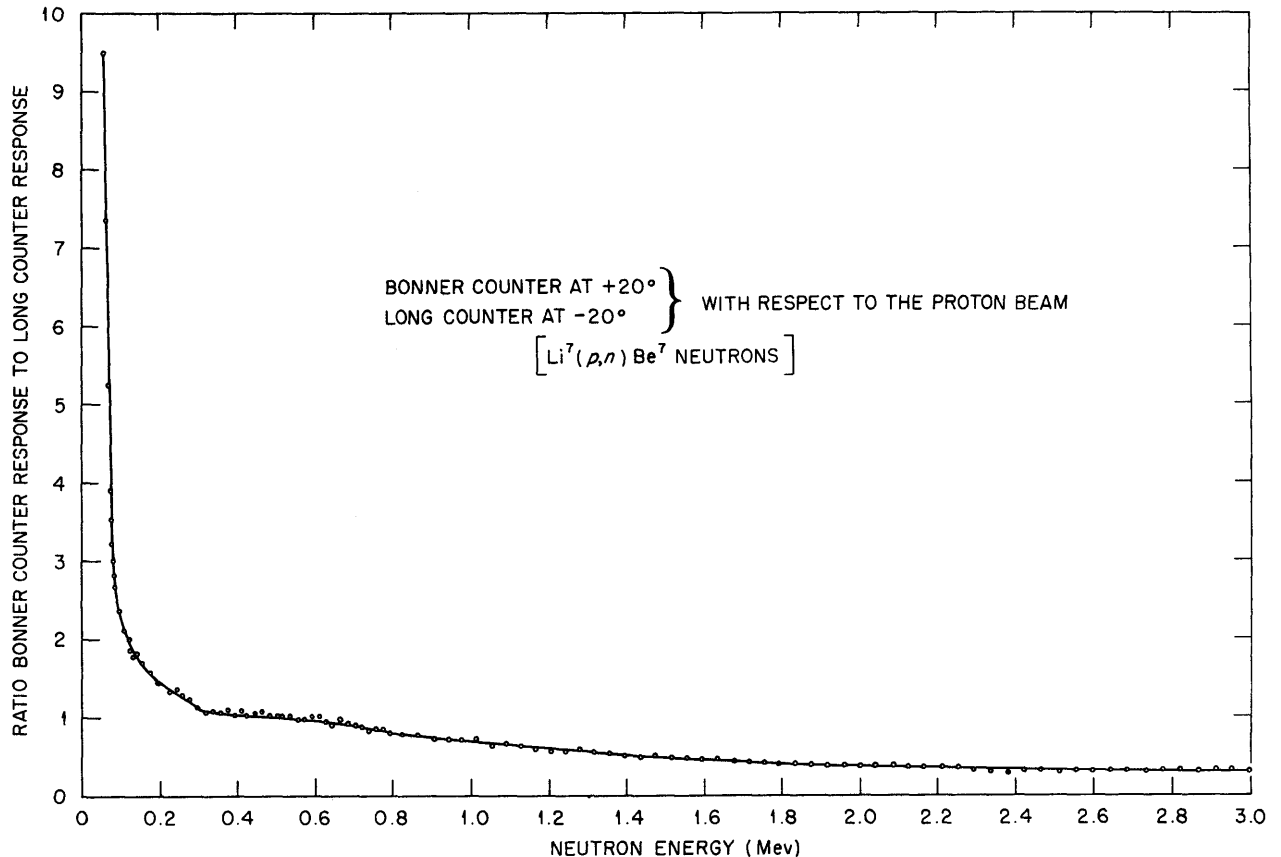


Fig. 5.2. Response of Bonner-Type Counter to Neutrons.

appears at 4.71 Mev (bombarding energies). The full width at half maximum of this new level is of the order of 0.5 Mev.

In order to determine levels in the residual nucleus, the Bonner counter was used to look for other neutron groups. No groups were found up to 5.3 Mev.

Be⁹(p,γ)B¹⁰ REACTION

J. K. Bair T. M. Hahn
 H. B. Willard J. D. Kington

The single-crystal NaI scintillation spectrometer has been set up and was

used to measure the yield of gamma rays from protons on beryllium for bombarding energies greater than 2.0 Mev. The counter was placed a few inches from the target in the forward direction and the output of the amplifier was fed through two discriminators to scalers so that gamma rays of energy above approximately 2.0 and 6.0 Mev were recorded separately. The curve corresponding to the high-energy gamma rays, corrected for background is shown in Fig. 5.4. From Figs. 5.3 and 5.4 it will be seen that the high-energy gamma rays and the neutrons show the same resonances. The respective full-level widths at half maximum are of the order of 75 and 200 kev.

PHYSICS DIVISION QUARTERLY PROGRESS REPORT

UNCLASSIFIED
DWG. 13695

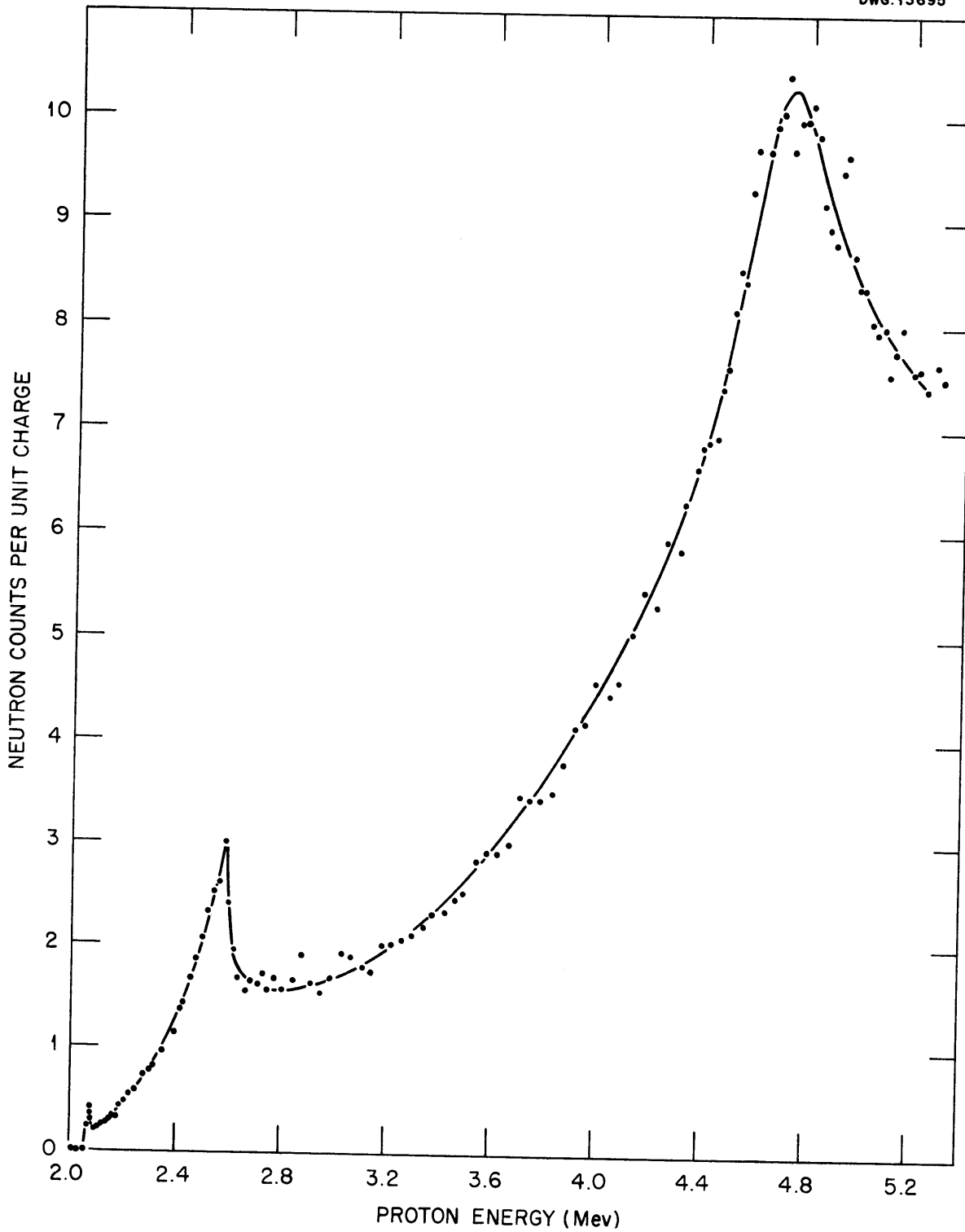


Fig. 5.3. $\text{Be}^9(p,n)\text{B}^9$ Yield (in the Forward Direction).

UNCLASSIFIED
DWG. 13696

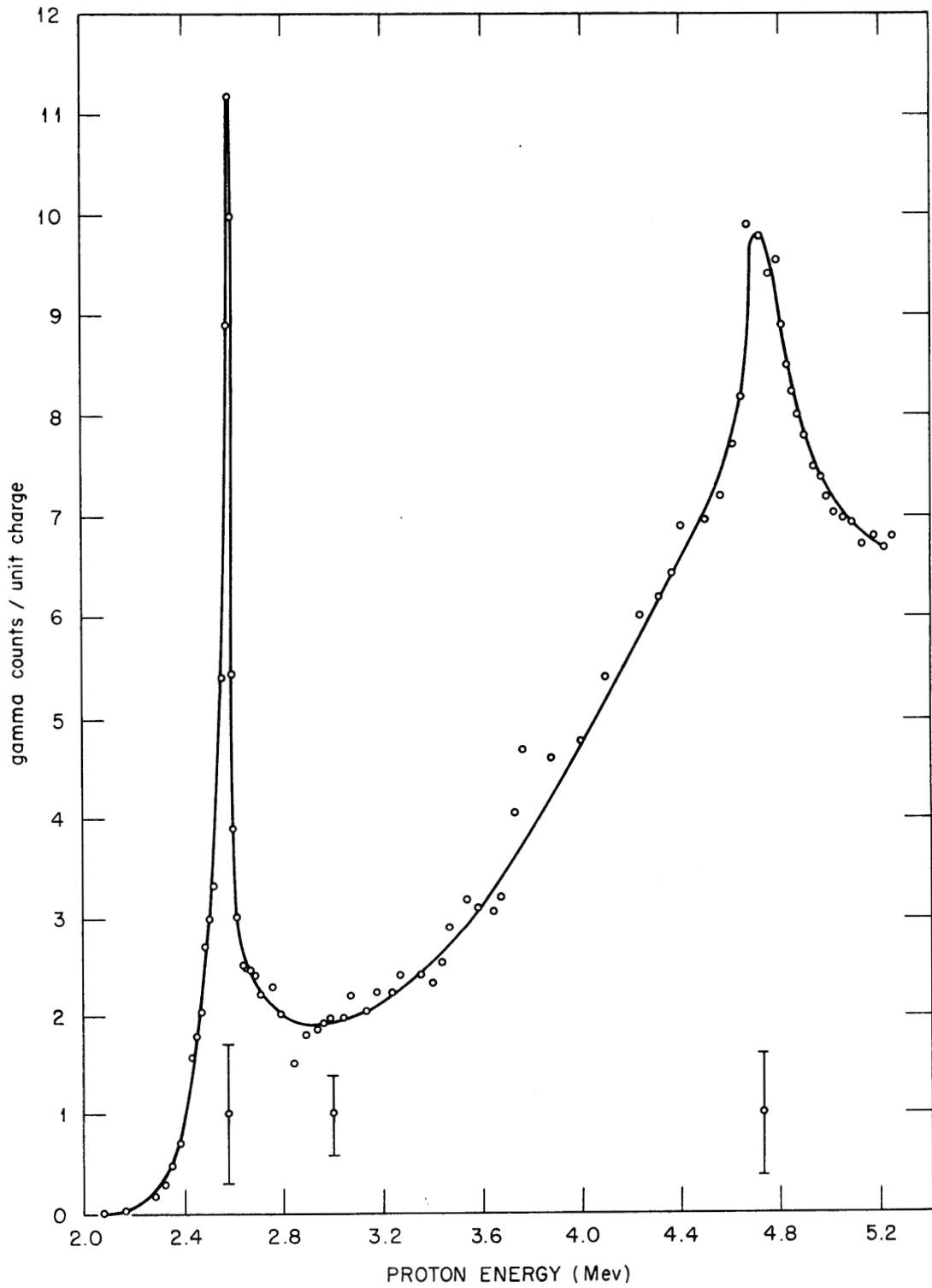
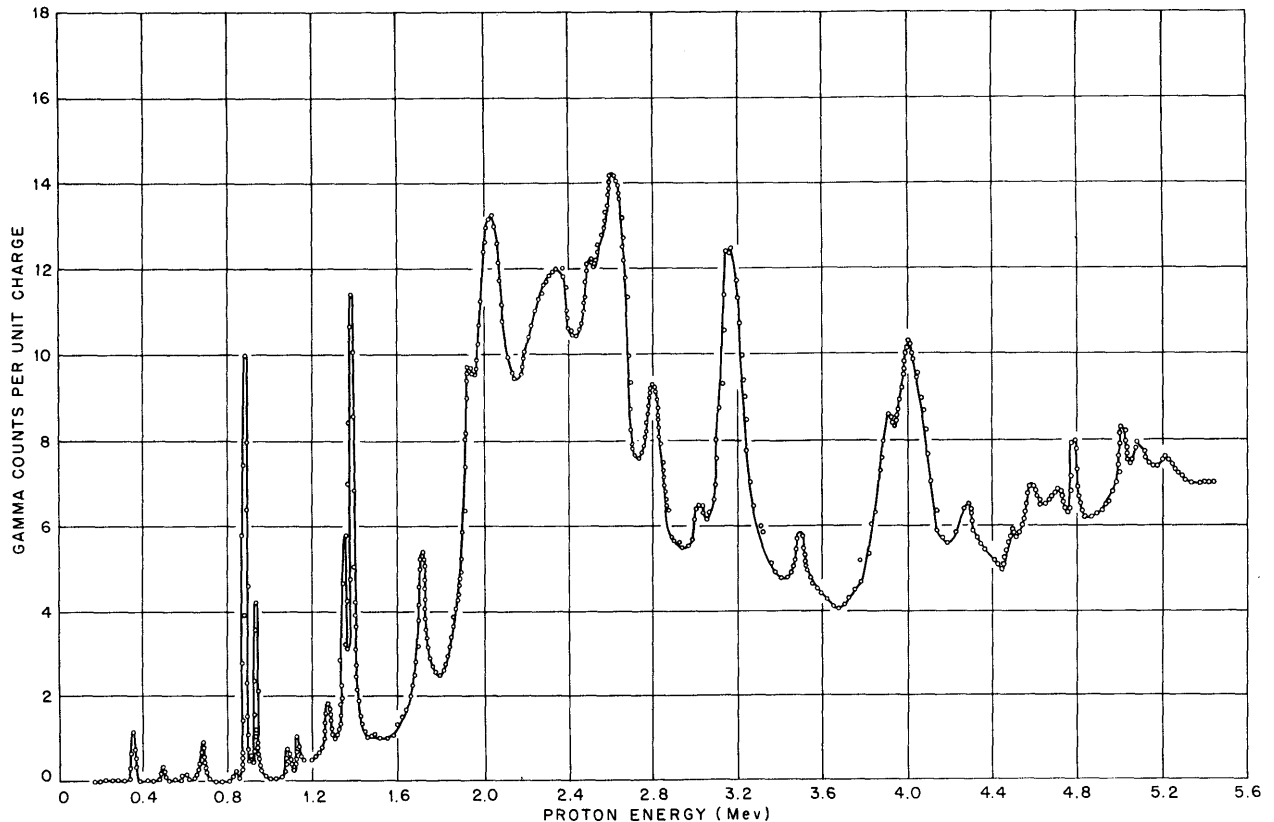


Fig. 5.4. $\text{Be}^9(p, \gamma)\text{B}^{10}$ Yield Curve (Gamma Rays Above ~ 6 Mev).

Fig. 5.5. $F^{19}(p,\gamma)$ Yield Curve

showed a nonisotropic angular distribution with respect to the beam in the center of mass (c.m.) system. In that experiment a proportional counter was used which was so biased that the background was negligible. Absorbers of aluminum were used to slow the protons down to approximately the end of their range so that the maximum height of pulse was obtained from the counter. It was found that for the bias setting adopted, several mils of absorber could be removed without a change in counting rate. Nevertheless, the margin was not as much as was desired in view of the 1.5 Mev or so variation in energy with angle due to c.m. motion. Also, there is a large spread in the pulse-height spectrum for protons of a

given energy. The angular distribution was, therefore, re-examined using a NaI crystal and photomultiplier as detector. The counting rate vs. bias had a long plateau which permitted setting the bias so as to count with confidence all protons regardless of angle. The angular distribution was studied in this way for several bombarding voltages up to 250 kev using a thick ZrD target. In each case the angular distribution turned out to be isotropic in the c.m. system to within 2%.

A further study has been made of the $He^3 + He^3$ reaction using a 1-mil aluminum foil as target and window, in the same arrangement reported

PHYSICS DIVISION QUARTERLY PROGRESS REPORT

UNCLASSIFIED
DWG. 13698

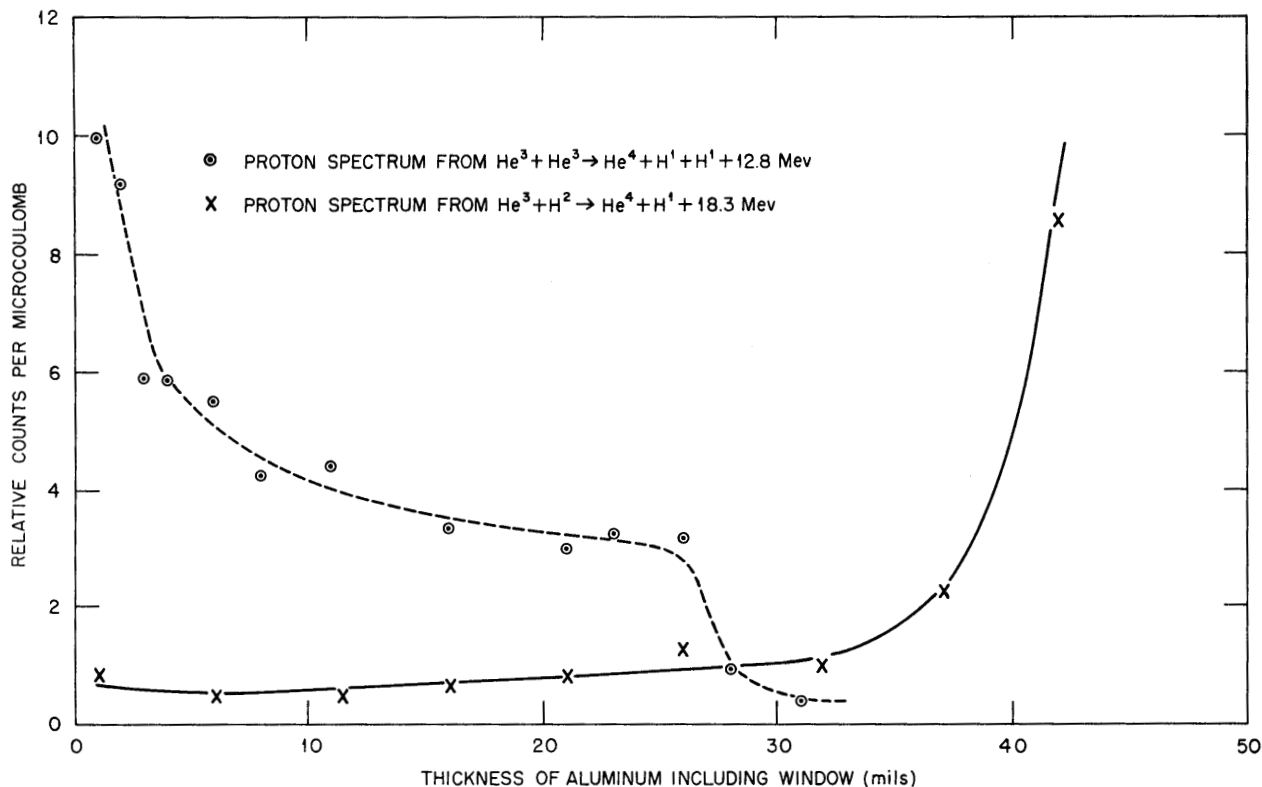


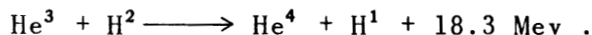
Fig. 5.6. Aluminum Absorption Spectrum with Biased Proportional Counter.

previously⁽¹¹⁾ where a 5-mil foil was used. The spectrum has been obtained, as previously, with a NaI spectrometer and also in the form of an absorption curve in aluminum using a proportional counter biased to count protons at the end of their range.

The part of the investigation reported here was primarily intended to accomplish three things: to get better statistics by more accurately holding the beam on the small spot which is the target; to show that the reaction being observed cannot be a secondary one produced by the 16-Mev protons from



and to try to resolve some apparent differences between the results obtained with the NaI spectrometer and the absorption in aluminum. Figure 5.6 shows the spectrum by the absorption in aluminum technique. On this figure is shown also a study of the protons from



The results show beyond doubt that the 16-Mev protons cannot be responsible for the spectrum that results from bombarding a clean aluminum foil with He³. It might be thought that the build-up of the He³ + He³ reaction with time was sufficient to identify the reaction, but under some circumstances H² can

⁽¹¹⁾W. M. Good, W. E. Kunz, and C. D. Moak, "The Reactions of He³ + He³," *Phys. Rev.* 83, 845 (1951).

INSTRUMENTAL DEVELOPMENTS

R. W. Lamphere C. H. Johnson
G. P. Robinson, Jr.

also build up on the clean aluminum target. Hence, the existence of a build-up is not in itself conclusive. The apparent rise in the number of protons at low energy is certainly partly instrumental. The proportional counter registers protons in a fixed energy range in the counter. However, this fixed energy range in the counter corresponds to an energy spread that increases as the energy of the proton incident on the absorber decreases. Uncertainty as to the exact energy interval to which the proportional counter responds makes the correction for this effect uncertain. Therefore Fig. 5.7 gives a more easily interpreted result for the spectrum and indicates comparable numbers of protons down to those just capable of penetrating the 1-mil window. Statistics are still too poor to show structure to the spectrum, and work continues to improve these by overcoming the present uncertainty of hitting the target.

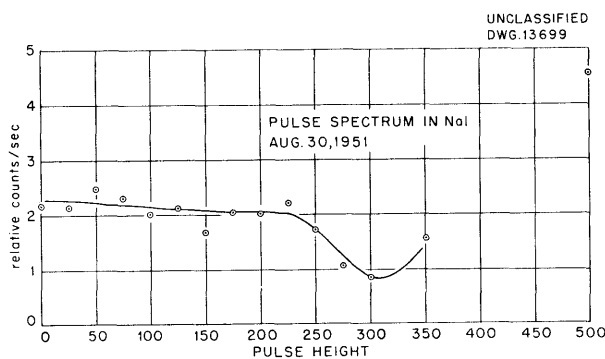


Fig. 5.7. Proton Spectrum from the $\text{He}^3 + \text{He}^3$ Reaction.

(12) C. D. Moak, H. Reese, Jr., and W. M. Good, "Design and Operation of a Radio-Frequency Ion Source for Particle Accelerators," *Nucleonics* 9, No. 3, 18 (1951).

The 2-Mv Van de Graaff which was originally built at M.I.T. as an electron accelerator has been converted to a proton accelerator. It has been successfully operated at 2.6 Mv without electron loading of the 56-in. accelerator tube. At 1.5 Mv an analyzed proton current of $100 \mu\text{a}$ was obtained using the r-f ion source developed here by Moak, Reece, and Good.⁽¹²⁾ Voltages were measured using a generating voltmeter calibrated with the well-known $\text{F}^{19}(p, \gamma)$ resonances.

As a preliminary experiment, the gamma-ray spectrum from proton capture on C^{12} was studied with a NaI scintillation spectrometer at the 0.456-Mev proton resonance. A single gamma ray was observed whose energy is 2.38 ± 0.03 Mev, which is in good agreement with the value of 2.37 ± 0.02 Mev determined from the resonance energy⁽¹³⁾ and the most recent mass values.⁽¹⁴⁾

At the present time equipment is not available for precision measurement and stabilization of the generator voltage, but work is in progress to provide precise control. In the meantime the experiments on proton resonance capture are being continued.

(13) W. A. Fowler and C. C. Lauritsen, "Gamma-Radiation from Light Nuclei under Proton Bombardment," *Phys. Rev.* 76, 314 (1949).

(14) C. W. Li, W. Whaling, W. A. Fowler, and C. C. Lauritsen, "Masses of Light Nuclei from Nuclear Disintegration Energies," *Phys. Rev.* 83, 512 (1951).

PHYSICS DIVISION QUARTERLY PROGRESS REPORT

6. NEUTRON-DIFFRACTION STUDIES

TOTAL NEUTRON CROSS SECTIONS AT INDIUM RESONANCE ENERGY (1.44 ev)

L. A. Rayburn E. O. Wollan

To obtain information about the spin-dependent scattering amplitudes for nuclei at thermal energies, measurements of both the coherent and the free scattering cross sections are required. In many cases for which coherent values are available, values for the free nuclear cross sections have not been accurately measured. For substances having not too large absorption, the free scattering cross section can be obtained by measurement of the transmission at neutron energies of the order of 1 ev or greater.

Equipment for using the method of indium resonance detection has been set up so that such measurements can be made on a somewhat routine basis. A flat-foil method with accurately reproducible geometry is used with an indium-lead alloy foil (indium equivalent of 0.6 mils) as detector placed in a cadmium shield. To eliminate the effect of high-energy indium resonances, all measurements

are made as a difference between indium in cadmium and indium covered by indium in cadmium. The primary beam is constantly monitored by a BF₃ counter. Measurements are made with and without sample, but after accurately correlating the direct beam measurements with the monitor these measurements need only be made from time to time as a check on the monitor. All samples are made to have nearly the same attenuation, which has the effect of reducing any errors that might arise from scattered radiation reaching the detector. Some preliminary results are given in Table 6.1.

MAGNETIC STRUCTURES OF V, Cr, Cb, Mo, and W

C. G. Shull M. K. Wilkinson

Neutron-powder-diffraction patterns have been obtained for pure samples of V, Cr, Cb, Mo, and W at a series of reduced and elevated temperatures in an investigation of their possible magnetic structures. All of these metallic elements are members of transition-element series that possess

TABLE 6.1
Cross Sections at 1.44 ev

SAMPLE	σ_{total} (barns)	σ_c (0.025 ev) (Pile Oscillator measurements by H. Pomerance)	σ_c (1.44 ev)	σ_s
Lead	11.30 ± 0.05			11.30 ± 0.05
Graphite	4.67 ± 0.03			4.67 ± 0.03
Bismuth	9.14 ± 0.04			9.14 ± 0.04
Nickel	18.0 ± 0.1	4.50 ± 0.23	0.59	17.41 ± 0.1
Copper	8.25 ± 0.04	3.57 ± 0.18	0.47	7.78 ± 0.07
Iron (Armco)	11.70 ± 0.04	2.39 ± 0.12	0.31	11.39 ± 0.06
Thorium	13.28 ± 0.08	7.0 ± 0.35	0.92	12.36 ± 0.15

incomplete and unfilled d -shells. Thus vanadium and chromium are normally considered as possessing 3 and 5 electrons in the $3d$ shell; columbium and molybdenum, 4 and 5 electrons in the $4d$ shell; and tungsten, 4 electrons in the $5d$ shell. According to Hund's rule, the spins of all of these electrons (the d -shells are less than half full) should be parallel and the individual atoms should possess strong atomic magnetic moments. Neutron-diffraction patterns should show how large the atomic moments are and whether they exist in an oriented or randomly directed magnetic lattice. Zener and his colleagues have discussed this magnetic orientation in a series of *Physical Review* papers (January 1951 and later) and they feel strongly that all of these simple body-centered cubic lattices are antiferromagnetic in type.

Powder patterns for these materials were taken at room temperature and also at liquid hydrogen temperature (24°K) in order to develop any incipient magnetic structure. The hydrogen content in the samples was measured by W. Walkowitz of the Metallurgy Division and was kept low enough so that the hydrogen scattering would not interfere with the similar-appearing magnetic diffuse scattering. Very careful X-ray diffraction examination was made on all of the samples by B. S. Borie and R. M. Steele to ensure that weak chemical impurities would not confuse the interpretation of the neutron pattern in terms of possible weak magnetic reflections.

Coherent Antiferromagnetic Reflections. The patterns for V, Cb, Mo, and W showed no measurable coherent reflections at other than the usual body-centered cubic reflection positions and these could be explained satisfactorily on the basis of nuclear scattering. From the sensitivity of

observation in the various patterns, an upper limit can be placed on the presence of the (100) antiferromagnetic reflection (the strongest to be expected), and consequently an upper limit on the strength of the aligned moments can be established. For vanadium, columbium, and tungsten this turns out to be 0.15, 0.3, and 0.4 Bohr magnetons, respectively. That for molybdenum should be about the same as for columbium but is not given at present since additional patterns for this material are being obtained. All of these materials were studied at temperatures down to that of liquid hydrogen (24°K).

In contrast to the above, the pattern for chromium showed a weak but definitely measurable antiferromagnetic (100) reflection, and this was studied in some detail. It was found to be about 30% stronger at 24°K than at room temperature, and at temperatures above the latter was found to decrease sharply. After correcting the observed (100) intensity for second-order wavelength ($\lambda/2$) contribution from the nuclear (200) reflection, the resultant antiferromagnetic intensity expressed in absolute scattering cross section units was calculated and is shown in Fig. 6.1 as a function of temperature. The temperature variation was found to be completely reversible and to represent a normal Curie temperature behavior, with a suggested Curie temperature somewhat above room temperature. Interestingly, changes in electrical resistivity, internal friction, coefficient of expansion, and Young's modulus for chromium have been reported⁽¹⁾ as occurring in the temperature vicinity of 50°C . Very careful X-ray diffraction studies were made

⁽¹⁾M. E. Fine, E. S. Greiner, and W. C. Ellis, "Transitions in Chromium," *Journal of Metals*, 191, 56 (1951).

PHYSICS DIVISION QUARTERLY PROGRESS REPORT

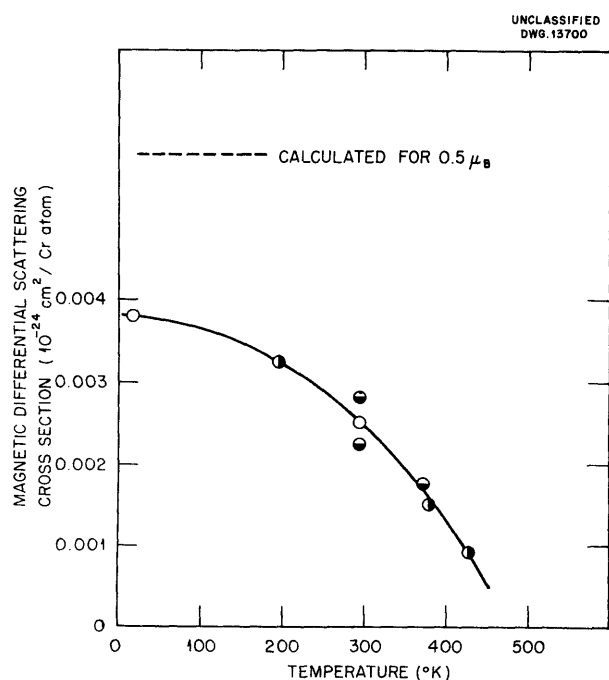


Fig. 6.1. Variation of Chromium Antiferromagnetic Intensity with Temperature.

in the vicinity of the (100) reflection, and it was established that there was no chemical impurity or lattice-defect type of scattering contributing to the observed neutron reflection. Using the low-temperature saturation cross section of 0.0038 barns per chromium atom, the effective magnetic moment of the antiferromagnetically coupled atoms is evaluated as 0.40 Bohr magnetons. This moment strength is very much less than the value of 5 Bohr magnetons, which would be obtained if there were 5 electrons in the 3d shell with parallel spins.

Magnetic Diffuse Scattering. Since the patterns show little or no aligned magnetic moment component, it is of interest to look for the effect of unaligned components. Unaligned moments should contribute to the diffuse scattering and this should be distinguishable by the angular variation of the magnetic form factor.

As typical of this investigation there is shown in Fig. 6.2 the observed diffused scattering (to the same scale) for the assigned atomic-spin quantum numbers. It is seen that there can exist very little, if any, of the angularly dependent magnetic scattering within the observed pattern. A calculation for the chromium data suggests that the unaligned moments cannot have a strength greater than about 0.1 Bohr magnetons. For the other members of the series, there is again no suggestion of magnetic diffuse scattering and the unaligned magnetic moments must be correspondingly small.

General Conclusions. The complete absence of magnetic scattering for V, Cb, Mo, and W and its weakness for Cr indicates the absence or weakness of the atomic magnetic moments in these materials. In turn this signifies that the assignment of a definite number of electrons in the 3d-shell of a particular atom has no justification or else, according to established spectroscopic rules, strong moments either aligned or unaligned with respect to neighbors should have been observed. This nonlocalization of the 3d electrons is just what is predicted by a collective electron or band-theory picture of the metallic structure by Pauling's molecular orbital viewpoint of metallic structures. Both methods of treatment have been used to account satisfactorily for the saturation magnetization of the ferromagnetic elements and their alloys. By extrapolation to the neighboring nonferromagnetic elements (Mn, Cr, and V) for which magnetic moment data are not available from magnetic studies, the theory predicts a small magnetic moment of 0.2 μ_B for chromium and zero moment for vanadium. As discussed previously, the neutron-scattering experiments show an antiferromagnetically coupled moment of 0.4 μ_B for chromium and no measurable

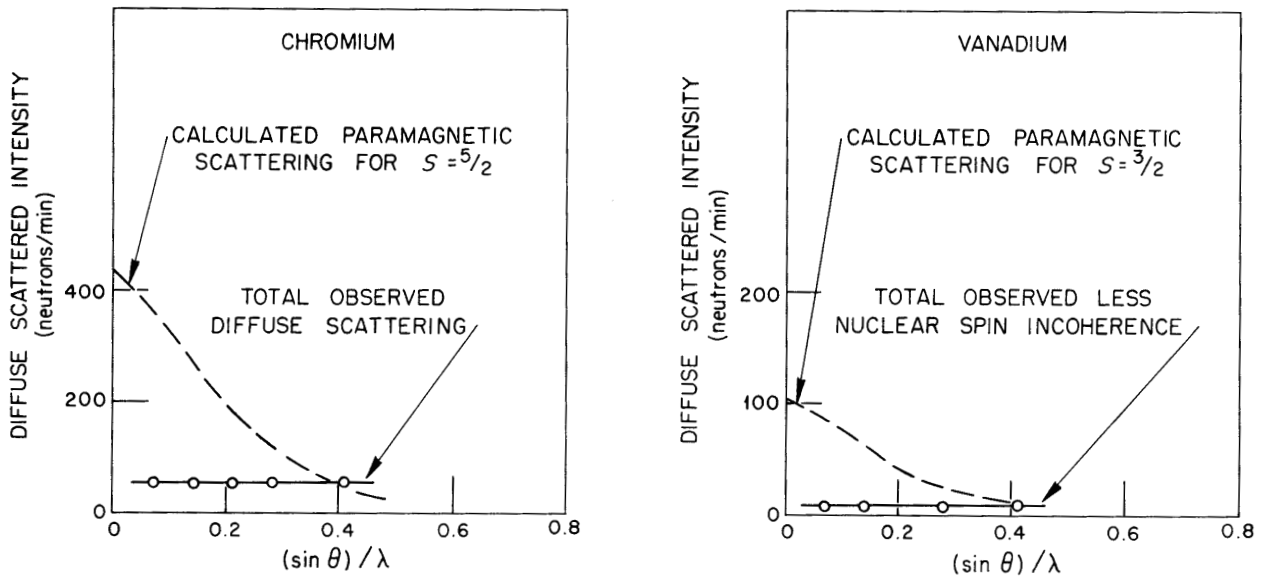


Fig. 6.2. Diffuse Neutron Scattering from Chromium and Vanadium.

moment for vanadium, and these can be considered in good agreement with the theory. Similar considerations for the members of the higher transition-element series, where the $4d$ and $5d$ shells are being filled, lead to predictions of very small or absent magnetic moments in Mo, Cb, and W, again in agreement with the scattering observations.

The theoretical predictions for the case of manganese for which the magnetic

moment should be about $1.2 \mu_B$ would be extremely interesting to study. There are imposing experimental problems here, however, since the crystallographic structure is very complex (with 58 atoms per unit cell) and it is not sure how significantly the neutron pattern can be treated quantitatively. It has been found difficult to interpret even the X-ray intensities for this crystal. An attack, however, on the manganese magnetic structure will be made.

PHYSICS DIVISION QUARTERLY PROGRESS REPORT

7. A CRYSTAL SPECTROMETER AS A SOURCE OF MONOENERGETIC THERMAL NEUTRONS

R. G. Allen T. E. Stephenson
T. I. Arnette

The use of a crystal spectrometer as a source of monoenergetic neutrons has been limited to the region of energies greater than about 0.03 eV due to the presence of higher-order reflections from the crystal as given by Bragg's Law,

$$n\lambda = 2d \sin \theta ,$$

where $n = 1, 2, 3, \dots$, order number.

Sturm⁽¹⁾ has described a method of correcting for the presence of higher orders by measuring the transmissions of a series of filters of known properties in the region of interest. However, by making use of the total reflection properties of mirrors^(2,3) for neutrons incident at very small glancing angles, it is possible to eliminate higher order reflections in the beam from the crystal. Thus, the range in which a crystal spectrometer can be used in a straight forward manner can be extended to much lower energies — around 0.005 eV and lower, depending upon the intensity available in this energy region.

The arrangement of the spectrometer and mirrors used for this purpose is shown schematically in Fig. 7.1. The detector is a BF_3 proportional counter with the boron enriched in the isotope B^{10} . In addition, a small BF_3 counter

tube was used to monitor the beam in order to correct for fluctuations in reactor intensity. These counter tubes were used with the usual associated electronic equipment.

The performance of the mirrors and their effect in eliminating high-order reflections is shown in Figs. 7.2 and 7.3.

Transmission measurements of total neutron cross sections as a function of neutron wavelength were made with this equipment in the standard way for indium, gold, and silver. A sample whose physical properties were known was prepared in a size large enough to intercept the entire beam. Measurements were taken of the beam intensity with and without the sample in the beam, along with measurements of the background intensity with and without the sample. Figure 7.4 and Table 7.1 give the results of these measurements with the solid lines obtained by fitting the data using the method of least squares. Sufficient data was taken so the statistical error in cross section was about 1%.

In order to see the effect of high orders on the total cross section, measurements were made on gold with and without the mirrors with the results given by Fig. 7.5. Figure 7.6 shows the crystalline scattering effects that are superposed on the $1/v$ capture cross section by the (311) planes in gold.

In general, the results of these measurements agree favorably with the cross sections that have been previously reported for this energy region. There

(1) W. J. Sturm, *Measurement of Neutron Cross Sections with a Crystal Spectrometer*, Argonne National Laboratory, MDDC-735 (1947).

(2) E. Fermi and L. Marshall, *Interference Phenomena of Slow Neutrons*, Argonne National Laboratory, MDDC-713 (1947).

(3) M. L. Goldberger, F. Seitz, and E. P. Wigner, *Theory of the Refraction and the Diffraction of Neutrons by Crystals*, Clinton Laboratories, MDDC-463 (1946).

UNCLASSIFIED
DWG. 13702

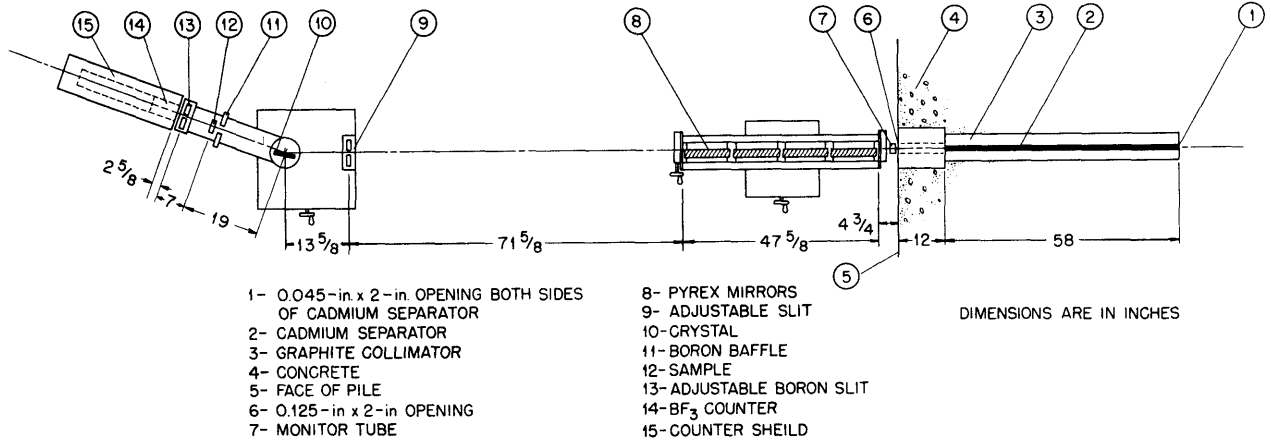


Fig. 7.1. Mirror and Spectrometer Diagram.

TABLE 7.1

Total Cross Sections of Indium, Gold, and Silver at Low Neutron Energies

ELEMENT	EQUATION OF $\sigma_t = f(\lambda)$	TOTAL SCATTERING CROSS SECTION (barns)
Indium	$\sigma_t = (99.71 \pm 0.37) \lambda + (20.39 \pm 0.95)$	20.39 ± 0.95
Gold	$\sigma_t = (52.24 \pm 0.34) \lambda + (11.17 \pm 0.82)$	11.17 ± 0.82
Silver	$\sigma_t = (34.98 \pm 0.34) \lambda + (5.89 \pm 0.85)$	5.89 ± 0.85

are some differences, however, particularly in the case of silver. Havens and Rainwater⁽⁴⁾ give the equation for total cross section of silver in the $1/v$ region as

$$\sigma_t = (31.64 \pm 0.35) \lambda + (6.6 \pm 0.5),$$

with λ expressed in Angstrom units, whereas the present measurements give

$$\sigma_t = (34.98 \pm 0.34) \lambda + (5.89 \pm 0.85).$$

(4) W. W. Havens and J. Rainwater, "The Slow Neutron Cross Sections of Indium, Gold, Silver, Antimony, Lithium, and Mercury as Measured with a Neutron Beam Spectrometer," *Phys. Rev.* 70, 154 (1946).

This difference in slope gives values of σ_t , measured by this method, that are about 8% to 10% greater than those reported by Havens and Rainwater.

The cross sections measured for indium agree very well with those measured by Borst *et al.*,⁽⁵⁾ using a crystal spectrometer, at high energies in the $1/v$ region. However, a greater slope, determined by these measurements, gives rise to cross sections

(5) L. B. Borst, A. J. Ulrich, C. L. Osborne, and B. Hasbrouck, "Neutron Diffraction and Nuclear Resonance Structure," *Phys. Rev.* 70, 557 (1946).

PHYSICS DIVISION QUARTERLY PROGRESS REPORT

UNCLASSIFIED
DWG. 13703

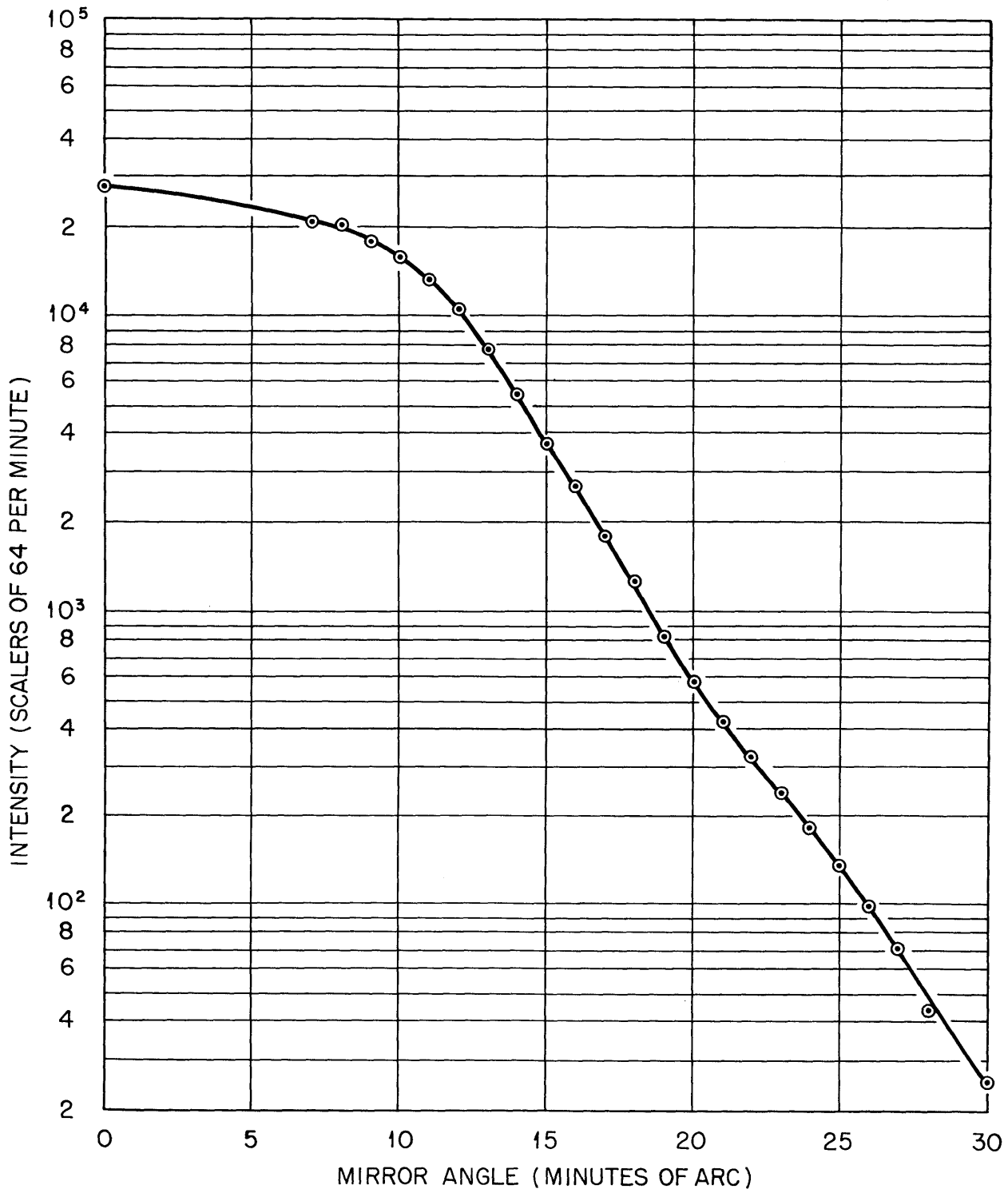


Fig. 7.2. Intensity Reflected from Mirror as a Function of Mirror Angle.

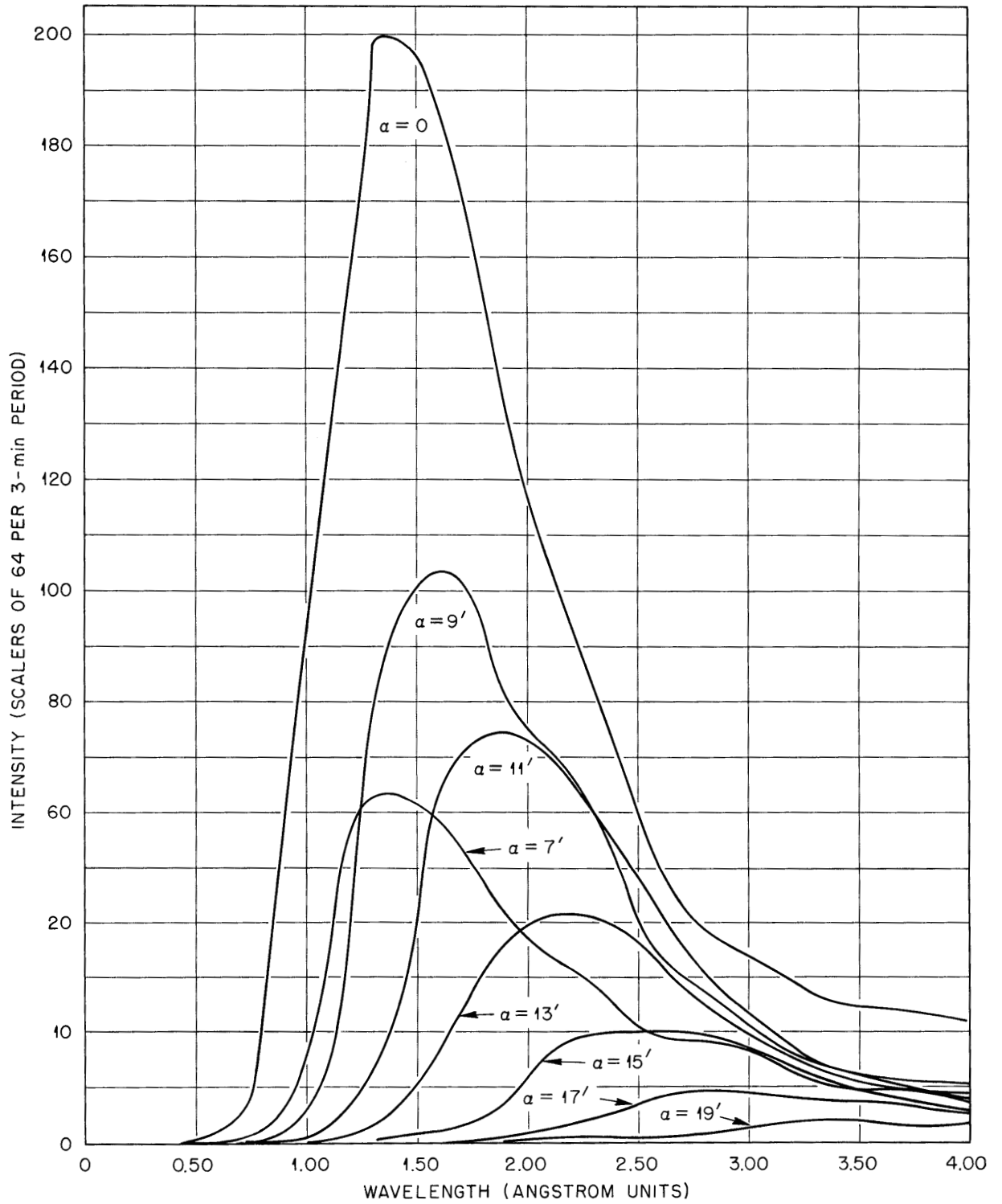


Fig. 7.3. Intensity Reflected from Mirror and Quartz Crystal as a Function of Neutron Wavelength for Various Mirror Angles (α).

PHYSICS DIVISION QUARTERLY PROGRESS REPORT

UNCLASSIFIED
DWG. 13705

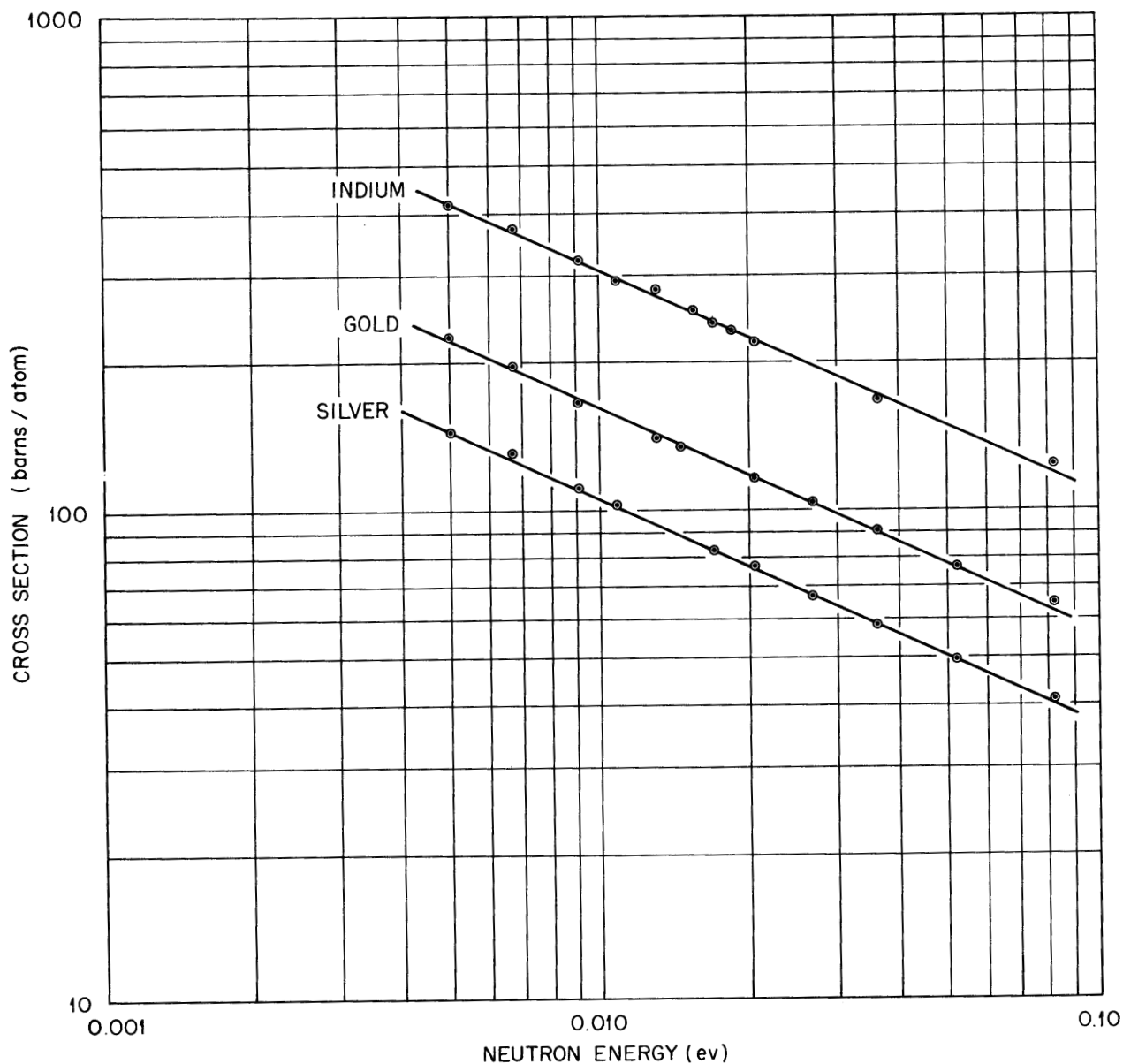


Fig. 7.4. Total Cross Section of Indium, Gold, and Silver as a Function of Neutron Energy.

that are about 8% higher at 0.005 eV than those that would be obtained by an extrapolation of Borst's data.

The values of the total cross section of gold are in very good agreement with those reported by others.⁽⁶⁾ The capture cross section at 0.025 eV

agrees to within less than 1% with that used by Pomerance⁽⁶⁾ as a standard in his work on capture cross sections.

⁽⁶⁾H. Pomerance, "Capture Cross Section of the Elements as Determined with Pile Oscillator," *Physics Division Quarterly Progress Report for Period Ending December 15, 1949*, ORNL-577, p. 25 (Feb. 8, 1950).

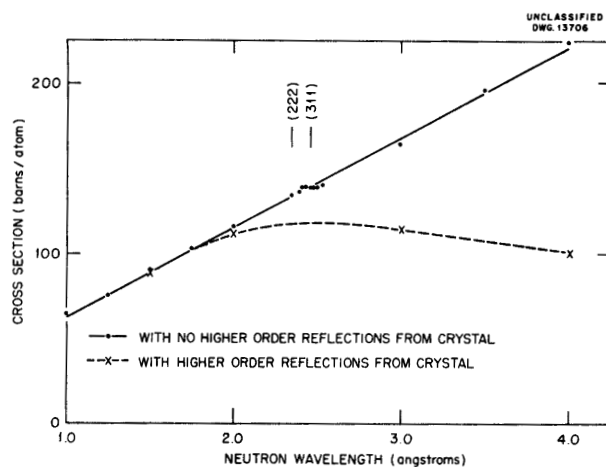


Fig. 7.5. Total Cross Section of Gold.

However, the total scattering cross section is higher than other reported values, ranging from 5 to 50% higher in the extremes.

Work is in progress using this equipment and materials that are predominately scatterers, with the purpose of determining coherent scattering cross sections from the heights of the discontinuities occurring in the measured total cross

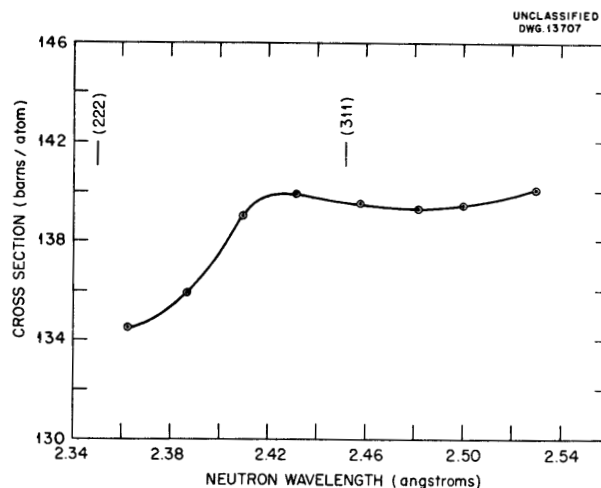


Fig. 7.6. Total Cross Section of Gold in the Region About the (311) Discontinuity.

section at those wavelengths satisfying the relation $\lambda = 2d_{hkl}$, where d_{hkl} is the (hkl) plane spacing in the scattering material.^(7,8)

(7) C. P. Stanford, *The Total Neutron Cross Sections of Ni⁵⁸ and Ni⁶⁰*, Thesis, ORNL-875 (Dec. 11, 1950).

(8) O. Halpern, M. Hamermesh, and M. H. Johnson, "The Passage of Neutrons Through Crystals and Polycrystals," *Phys. Rev.* 59, 981 (1941).

PHYSICS DIVISION QUARTERLY PROGRESS REPORT

8. LOW-TEMPERATURE PHYSICS

L. D. Roberts C. C. Sartain
J. W. T. Dabbs, Jr.

SPECIFIC HEAT OF NEODYMIUM ETHYL SULFATE AND OF NEODYMIUM SULFATE FROM 1 TO 2°K

It has been suggested by Casimir and others that the properties of suitable paramagnetic salts for a region of T below 1°K can be described in terms of a parameter, b/C , the ratio of the specific heat constant b to the Curie constant C , where b is defined by the equation $C_I = b/T^2$, with C_I the specific heat at constant magnetization and T the absolute temperature. This has been confirmed for a number of salts, and b/C is thus an important parameter of low-temperature physics. Measurements have been made of b/C for two samples of $\text{Nd}(\text{C}_2\text{H}_5\text{SO}_4)_3 \cdot 9\text{H}_2\text{O}$ in the temperature region from 1 to 2°K. Sample I was prepared from neodymium of normal isotopic composition, and sample II was prepared from neodymium highly enriched in Nd^{143} . Measurements are under way on a sample highly enriched in Nd^{142} . By multiplying the measured values of b/C for each of the three samples by the Curie constant C , the respective specific heat constants b are obtained. When these b 's are suitably combined, the electron spin interaction contribution to the specific heat, b_e/T^2 , and the hyperfine splitting contribution to the specific heat, b_n/T^2 , for both Nd^{143} and Nd^{145} may be obtained. From the completed measurements on samples I and II and from the ratio of the hyperfine splitting of Nd^{143} and Nd^{145} as given by Bleaney and Scovil,⁽¹⁾ b_e is found to be of the order of magnitude that

may be expected from Van Vleck's theory, and the b_n so obtained for Nd^{143} compares well with the value computed from microwave measurements by Bleaney and Scovil.

Theory. Following the treatment of Benzie and Cook⁽²⁾ and of Casimir,⁽³⁾ the specific heat C_I is given by

$$C_I = \frac{CT}{(T - \beta)^3} \frac{X_s}{X_T - X_s} H^2, \quad (1)$$

where C is the Curie-Weiss constant, X_T and X_s are the isothermal and adiabatic differential magnetic susceptibilities, respectively, and H is an applied constant magnetic field. At zero magnetic field, $H = 0$, $X_T = X_s$; and when a field, H , is applied, X_T remains constant within a small saturation correction of less than one part per thousand in this work and this correction is neglected. On the other hand, X_s is, in general, a function of the magnetic field, the electron spin-lattice relaxation time, the specific heat C_I due to electron spin interactions, and the specific heat of the lattice along with the sample support, etc. By not immersing the sample in liquid helium, as is often done, the effect of the specific heat of the surroundings of the sample is minimized, and by measuring X_s at sufficiently high frequencies, relaxation time effects can be made negligible. In these

⁽¹⁾B. Bleaney and H. E. D. Scovil, "Nuclear Spins of Neodymium 143 and 145," *Proc. Phys. Soc. (London)* A63, 1369 (1950).

⁽²⁾R. J. Benzie and A. H. Cooke, "Specific Heats of Some Paramagnetic Salts at Temperatures near 1°K," *Proc. Phys. Soc. (London)* A63, 213 (1950).

⁽³⁾H. B. G. Casimir, *Magnetism and Very Low Temperatures*, Cambridge (Eng.) The University Press, 1940.

experiments, χ_s is shown experimentally to be independent of the frequency in the range from 360 to 1200 cycles per second. This is taken as sufficient evidence that χ_s is a function of H only in this frequency range, and that the measured χ_s is the χ_s of Eq. 1.

For neodymium ethyl sulfate Van Den Handel and Hupse⁽⁴⁾ have shown that $\beta = 0$. Assuming also that the specific heat at 1 to 2°K may be described by

$$C_I = \frac{b}{T^2}, \quad (2)$$

Eq. 1 reduces to

$$\frac{b}{C} = \frac{\chi_s}{\chi_T - \chi_s} H^2. \quad (3)$$

Equation 3 was used to interpret this data.

The two important contributions to the Hamiltonian describing neodymium ethyl sulfate in the temperature region 1 to 2°K, are the hyperfine structure coupling of the electron spin with the nuclear spin within a given atom, and the dipole-dipole interaction and exchange interaction of the electron spins of different atoms in the lattice. The Hamiltonian for the salt is then

$$\mathcal{H} = AI_x S_x + B(I_y S_y + I_z S_z) + P(S). \quad (4)$$

The first two terms on the right are the contribution to the Hamiltonian due to hyperfine coupling as given by Bleaney and Scovil,⁽¹⁾ and the third term, $P(S)$, corresponds to electron dipole-dipole interaction and exchange

(4) J. V. D. Handel and J. C. Hupse, "The Magnetic Susceptibilities of a Single Crystal of Neodymiumethylsulfate," *Physica* 9, 225 (1942).

as discussed by Van Vleck.⁽⁵⁾ It is easily shown that, approximately,

$$C_I = Nk \cdot \frac{1}{k^2 T^2} \text{Tr } \mathcal{H}^2, \quad (5)$$

where N is Avogadro's number and k is the Boltzmann constant.

$$\begin{aligned} \text{Tr } \mathcal{H}^2 &= \text{Tr}[AI_x S_x + B(I_y S_y + I_z S_z)]^2 \\ &+ \text{Tr}P^2(S) \\ &+ \text{Tr}[AI_x S_x + B(I_y S_y + I_z S_z)] P(S) \\ &+ \text{Tr}P(S) \cdot [AI_x S_x + B(I_y S_y + I_z S_z)]. \quad (6) \end{aligned}$$

Since $\text{Tr}I = 0$, Eq. 6 reduces to

$$\text{Tr } \mathcal{H}^2 = \text{Tr}[AI_x S_x + B(I_y S_y + I_z S_z)]^2 + \text{Tr}P^2(S).$$

Thus, the specific heat is

$$C_I = \frac{(b_n + b_e)}{T^2}, \quad (7)$$

$$b_e = \frac{N}{k} \text{Tr}P^2(S), \quad (8)$$

$$b_n = \frac{N}{k} \text{Tr}[AI_x S_x + B(I_y S_y + I_z S_z)]^2. \quad (9)$$

The latter trace has been evaluated by Bleaney⁽⁶⁾ giving

$$\begin{aligned} b_n &= \left[\frac{hc}{k} \right]^2 \left[\frac{1}{9} \right] (A^2 + 2B^2) \\ &\cdot S(S + 1) I(I + 1) Nk. \end{aligned}$$

(5) J. H. Van Vleck, "The Influence of Dipole-Dipole Coupling on the Specific Heat and Susceptibility of a Paramagnetic Salt," *J. Chem. Phys.* 5, 320 (1937).

(6) B. Bleaney, "Nuclear Specific Heats in Paramagnetic Salts," *Phys. Rev.* 78, 214 (1950).

PHYSICS DIVISION QUARTERLY PROGRESS REPORT

In this work $C_I T^2$ is measured for several samples of differing isotopic composition, and the corresponding simultaneous equations are solved for b_n and b_e .

Materials Used. The normal neodymium ethyl sulfate $\text{Nd}(\text{C}_2\text{H}_5\text{SO}_4)_3 \cdot 9\text{H}_2\text{O}$, sample I, was prepared by D. E. LaValle from neodymium oxide which was spectroscopically pure. The neodymium isotopic composition of this sample was assumed to be that given by Mattauch and co-workers, Table 8.1.

TABLE 8.1

Isotopic Composition of the Neodymium Used to Prepare the Samples

ISOTOPE	PER CENT ABUNDANCE		
	SAMPLE I	SAMPLE II	SAMPLE III
142	27.13	4.04	93.00
143	12.20	83.93	3.18
144	23.87	8.83	2.89
145	8.30	1.78	0.368
146	17.18	1.16	0.414
148	5.72	0.149	0.084
150	5.60	0.108	0.066

The neodymium ethyl sulfate, sample II, was prepared by R. H. Sampley of this laboratory from the oxide of the separated neodymium isotope Nd^{143} . This oxide and that used for sample III were also of spectroscopic purity. The isotope separation and mass analysis of samples II and III were performed by the Stable Isotopes Division of this laboratory. Their results for the mass analysis are tabulated in Table 8.1.

In addition to samples I and II, sample III of the ethyl sulfate was prepared from neodymium enriched in Nd^{142} . Sample III was inadvertently

decomposed to the sulfate, $\text{Nd}_2(\text{SO}_4)_3 \cdot 8\text{H}_2\text{O}$, however, the C_I measurements were made on this material also.

Each of the three samples was recrystallized three times. The last recrystallization in each case was performed immediately before the low-temperature measurements were made. The weights of the samples were as follows: sample I, 1.372 g; sample II, 1.985 g; sample III, 0.907 g.

The small crystals of salt investigated (about 1 mm^3 average size) were loosely pressed into a spherical lucite container, A, of 12.7 mm internal diameter. This was inserted into a glass tube, B. This tube was immersed in liquid helium, which was in turn contained in a liquid-nitrogen-jacketed Dewar flask. Thermal contact between the sample in A and the liquid helium surrounding tube B was maintained by helium gas at a pressure of about $50 \mu \text{ Hg}$. The advantage of using exchange gas to provide this thermal contact rather than directly immersing the sample in the liquid helium is that electron spin-lattice relaxation time effects are somewhat minimized.

The susceptibility of the salt was measured by means of the usual compensated-mutual-inductance, Hartshorn-bridge method. The steady fields, H , up to about 250 gauss were applied parallel to the alternating field from the Hartshorn-bridge current by use of battery-supplied current in an external iron-free solenoid.

Results. The measurements of b/C on each of the three samples were carried out at 360, 600, 900, and 1200 cycles at two temperatures. The data are recorded in Table 8.2. The b/C value given for each temperature is the average of the values for the four measurement frequencies with the average deviation given. The Curie constant per mole, $C = 0.674$, was

TABLE 8.2

Summary of the Specific-Heat Measurements

SAMPLE	TEMP. (°K)	$b/C \times 10^{-6}$	AVERAGE DEVIATION	$b/C \times 10^{-6}$ (average)	$b \times 10^{-6}$
I. Normal $\text{Nd}(\text{C}_2\text{H}_5\text{SO}_4)_3 \cdot 9\text{H}_2\text{O}$	1.101	0.176	0.002	0.178	0.120
	2.09	0.181	0.007		
II. $\text{Nd}^{143}(\text{C}_2\text{H}_5\text{SO}_4)_3 \cdot 9\text{H}_2\text{O}$	1.12	0.675	0.025	0.726	0.489
	2.20	0.777	0.046		
III. $\text{Nd}_2^{142}(\text{SO}_4)_3 \cdot 8\text{H}_2\text{O}$	1.08	0.138	0.005	0.139	0.0936
	2.19	0.140	0.006		

calculated from the g factors given by Bleaney and Scovil.⁽¹⁾

From the microwave work of Bleaney and Scovil⁽¹⁾ are obtained the values $b_n(\text{Nd}^{143}) = 0.546 \times 10^6 \pm 0.04 \times 10^6$ and $b_n(\text{Nd}^{145}) = 0.207 \times 10^6 \pm 0.016 \times 10^6$. From the data of Table 8.2 and the ratio of the above two numbers by Bleaney and Scovil,⁽¹⁾ the value $b_n(\text{Nd}^{143}) = 0.535 \times 10^6$ is obtained. The value obtained from specific-heat measurements agrees fairly well with the microwave result. Also, it is found that $b_e = 0.038 \times 10^6$ for neodymium ethyl sulfate and $b_e = 0.076 \times 10^6$ for neodymium sulfate. These values for b_e agree in magnitude with Van Vleck's⁽⁵⁾ theory. For example, for the ethyl sulfate the dipole-dipole interaction would calculate to $b_e = 0.023 \times 10^6$. Quantitative agreement is not expected since the theory is for the case of an isotropic g factor, whereas the g factor for the neodymium ion is very anisotropic.

Also, the calculated b_e does not take account of the exchange contribution.

Finally, it is interesting to note the relative size of b_n and b_e . In general, hyperfine structure coupling is found to be a small perturbation on other large interactions, and this is usually found to be true in the case of specific heats at low temperatures. For $\text{Nd}^{143}(\text{C}_2\text{H}_5\text{SO}_4)_3 \cdot 9\text{H}_2\text{O}$, however, the nuclear contribution to the specific heat is 14 times larger than all other contributions combined.

The work described in this section is being continued and it is believed that the salt, $\text{Nd}^{143}(\text{C}_2\text{H}_5\text{SO}_4)_3 \cdot 9\text{H}_2\text{O}$, will be especially suitable for nuclear alignment experiments.

HEAT LEAK STUDIES BELOW 1°K

A major problem in all work concerning adiabatic demagnetization has

PHYSICS DIVISION QUARTERLY PROGRESS REPORT

been the reduction of heat leaks to the cold demagnetized sample of paramagnetic salt. In certain cases the heat input must not exceed a few thousand ergs in experiments of several hours duration. A study of this problem has yielded several interesting results. These requirements must be met: radiation influx, residual helium gas, and sample-support conduction must all be minimized to obtain a small heat leak. It is easily shown that radiation from the sample tube walls (at 1°K) is only of the order of a few tenths of an erg per minute for usual size samples, and heat conduction along the thin nylon or cotton fibers used for the sample suspension is very small. Preferably, one should use single-strand fibers to minimize the possibility of outgassing.

A rather surprising result is obtained if the heat influx due to condensation of helium gas on the cold sample is calculated. If a "sticking coefficient," C_A , of unity and a heat of condensation of helium of ~ 16 cal/mole (0.4°K value⁽⁷⁾ for He) is assumed, the following may be written:

$$\dot{Q} = C_A A \cdot \frac{nv}{4} \cdot \frac{H_c}{N},$$

where

A is the sample surface area,

nv is the flux of helium atoms,

H_c/N is the heat of condensation per atom,

and nv is given by

$$nv = 0.13 \frac{p(\text{mm Hg})}{\sqrt{T}},$$

T being the gas temperature in °K; then at $T = 1^\circ\text{K}$, $A = 3 \text{ cm}^2$,

$$\dot{Q} (\text{erg/min}) \approx 3.8 \times 10^9 p(\text{mm Hg}).$$

Thus, a pressure of 10^{-9} mm Hg will cause a heat leak of ~ 5 erg/min to a typical sample.

Since heat leaks as small as 2 to 5 erg/min have been observed at this laboratory and elsewhere, it may be concluded that helium pressures as low as $\sim 10^{-9}$ mm Hg are obtained during a demagnetization under good conditions. It is to be noted that an ionization gage at the room-temperature end of the sample tube may give a reading of 1×10^{-6} mm Hg or even higher; however, even considering the role the salt sample plays in "cleaning up" the sample space, there is agreement with the idea of Sears,⁽⁸⁾ which has received rather strong confirmation by Berry,⁽⁹⁾ that the pumping speed of diffusion pumps is independent of the low pressure below a certain critical pressure, and that the partial pressure of helium on the low-pressure side is indeed several orders of magnitude lower than the ionization gage reading.

The situation outlined previously is not completely satisfactory in the case of a metallic sample tube of larger diameter (e.g., 1 in.) since there is another source of heat, i.e., radiation coming down the sample tube from the room-temperature end. Here one is confronted with "light piping" of long wavelength radiation

⁽⁸⁾G. W. Sears, "Ultimate Vacua of Diffusion Pumps," *Rev. Sci. Instr.* 20, 458 (1949).

⁽⁹⁾C. E. Berry, "Pumping Speed of Diffusion Pumps Below Limiting Pressure," *Rev. Sci. Instr.* 20, 835 (1949).

⁽⁷⁾W. H. Keesom, *Helium*, Elsevier, Amsterdam, New York, 1942.

(10 μ) past even fairly elaborate radiation shields. Two radiation shields such as that shown in Fig. 8.1 are quite adequate to secure a heat leak of ~ 5 erg/min in a glass sample tube, but four such shields in a metal tube give at best heat leaks of ~ 100 erg/min.

Experience indicates that in a metal sample tube it may be necessary to surround the sample with a holder such as that shown in the bottom part of Fig. 8.1 to prevent radiation leakage around the edges of the shields from reaching the sample; work on this problem has been started.

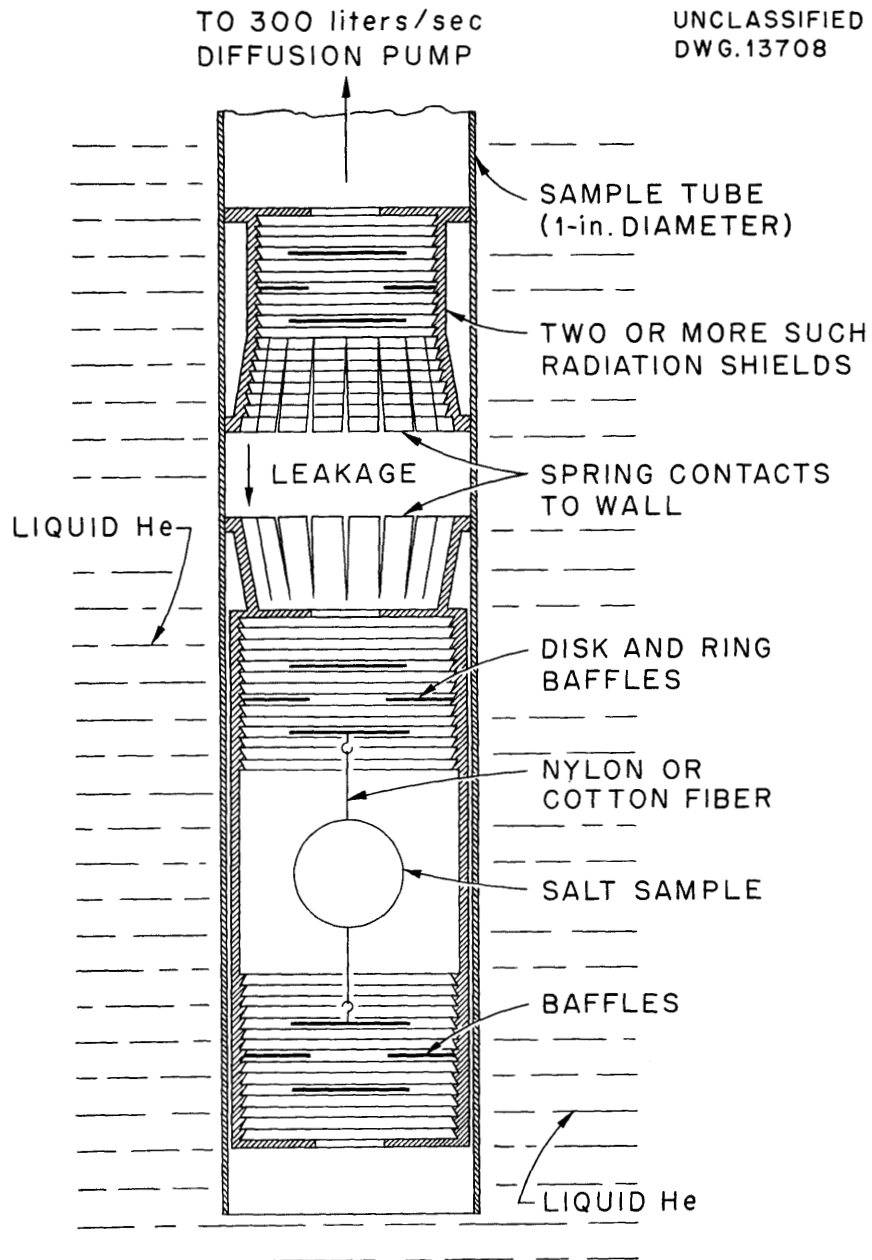


Fig. 8.1. Diagram of Shield Assembly to Reduce Radiation Heat Losses to Samples at Very Low Temperatures.

PHYSICS DIVISION QUARTERLY PROGRESS REPORT

9. STABLE-ISOTOPE CROSS SECTIONS

H. Pomerance

T. Arnette

The pile oscillator has been used to measure the thermal-neutron capture cross sections of stable separated isotopes procured from Y-12. The values are found by comparison with gold, which has a value of 95 barns for neutrons of 2200 m/sec (0.025 ev). The errors are estimates based on the sample size and the relative contributions from the other isotopes present in the samples. The mass assays were furnished by Y-12. Based on approximate quantitative spectrographic analyses, corrections for cadmium impurity (Ca^{40} , Ce^{142}), boron (Tl^{203} and Tl^{205}), and lithium ($\text{K}^{39,41}$) were made.

The atomic cross section is the contribution of the isotope to the natural element value, and is obtained by multiplying the nuclear (isotopic) cross section by the relative abundance in the natural element.

Final values of thermal-neutron capture cross sections follow:

ISOTOPE	ISOTOPIC CROSS SECTION (barns)	ATOMIC CROSS SECTION (barns)
Ce^{136}	25 ± 100%	0.05
Ce^{138}	9 ± 70%	0.02
Ce^{140}	0.63 ± 10%	0.56
Ce^{142}	1.76 ± 15%	0.20
Fe^{54}	2.3 ± 10%	0.14
Re^{185}	100 ± 8%	37.3
Re^{187}	63 ± 8%	39.6
Tl^{203}	11.0 ± 8%	3.20

(continued)

ISOTOPE	ISOTOPIC CROSS SECTION (barns)	ATOMIC CROSS SECTION (barns)
Tl^{205}	0.74 ± 10%	0.52
W^{180}	30 (factor of 4)	0.04
W^{182}	19.2 ± 10%	4.95
W^{183}	10.9 ± 10%	1.55
W^{184}	2.0 ± 15%	0.60
W^{186}	34 ± 8%	9.95

Tentative values:

Ca^{40}	0.45 ± 15%
Ca^{42}	38
K^{39}	1.4 - 2.1*
K^{41}	1.1 - 1.5*
Sr^{84}	~100

*Lithium impurity makes these values uncertain.

The comparison of the measured element cross sections with the value obtained by adding the atomic cross sections in this report shows differences within the estimated precision for three of the four cases:

ELEMENT	SUM OF ATOMIC VALUES (barns)	ELEMENT VALUE (barns)	DIFFERENCE (%)
Ce	0.83	0.80	3.8
Re	76.9	83.9	8.4
Tl	3.72	3.27	13.7
W	17.1	17.7	3.5

10. TIME-OF-FLIGHT SPECTROMETER

G. S. Pawlicki* E. C. Smith

Serious delays occurred in the fabrication of the rotor because of a brazing operation in assembly. The use of copper brazing was abandoned in favor of silver-copper eutectic alloy. The brazing was successfully completed in an improvised hydrogen-atmosphere furnace. At the present time the brazed subassembly is being finished-ground by an outside contractor who had previously ground the shroud ring for the rotor. When the

subassembly is returned the rotor will be assembled and balanced at the Laboratory. The present estimated completion date is October 26, 1951.

Visible progress on the installation work at the reactor occurred during the past quarter. The cast-concrete blast shield for the rotor is due for completion about October 3. The foundation and floor of the detector house are completed, and construction remaining to be done consists of erecting the detector house and installing the vacuum pipe for the neutron beam.

*ORINS fellow.

PHYSICS DIVISION QUARTERLY PROGRESS REPORT

11. HEAVY-ION RESEARCH

G. E. Evans C. F. Barnett
P. M. Stier V. L. DiRito

ION-SOURCE STUDIES

A Philips-ionization-gage type of ion source has been completed and installed on the Cockcroft-Walton accelerator. Total ion currents of 1 ma have been obtained at the source, giving about 500 μ a of resolved current at the target position. The maximum power consumption of the source is about 200 watts. Gas leakage from the source is quite small, allowing a normal operating pressure in the Cockcroft-Walton tube of about 2×10^{-5} mm Hg. In preliminary tests, hydrogen, helium, nitrogen, and argon ions have been accelerated. For argon ions, from one-half to three-fourths of the total beam is available as resolved A^+ ions.

SPECIFIC IONIZATION STUDIES

Specific ionization vs. range curves are being determined for argon ions in air in the energy region 20 to 200 kev. (The upper energy limit is at present set by the available magnetic field in the magnetic analyzer.) This experiment is a part of a general program to study the influence upon specific ionization of such factors as mass and type of incident

ion, charge of incident ion, energy of the incident ion, and nature of the stopping gas. Preliminary results for low-energy argon ions indicate very small values of specific ionization, on the order of magnitude of several hundred ions per millimeter of air at normal temperature and pressure.

The ionization chamber and associated instruments have been checked by measuring the extrapolated ionization range of protons of varying energy (20 to 350 kev) in air. Results of measurements made on different days with varying gas pressures, different ion chambers, and different beam intensities agree well when corrected to normal temperature and pressure, indicating satisfactory reproducibility in the experimental equipment.

PARTICLE DETECTION

An electron multiplier of the Allen design using beryllium-copper dynodes is being tested to determine its efficiency for the counting of low-energy heavy ions. It is planned to study the dependence of average pulse height upon mass and energy of the incident particles.

12. STANDARD PILE

E. D. Klema

The data from the diffusion-length measurements have been calculated and a report of these experiments has been written.

The NaI scintillation counter has been used to make an absolute measurement of the activity of a gold foil in slot No. 11 of the standard pile. The counter was calibrated by means of the high-pressure ion chamber in the Chemistry Division, which in turn was standardized with a beta-gamma coinci-

dence apparatus in the Chemistry Division.

The preliminary experiments have been completed, and the final measurements are being made. From them a value of the thermal neutron flux in slot No. 11 will be calculated. It is planned to determine the thermal flux in other slots of the standard pile by means of ratio measurements with cadmium-covered and bare indium foils.

PHYSICS DIVISION QUARTERLY PROGRESS REPORT

13. THEORETICAL PHYSICS

In the main, work in the theoretical physics group has been concerned with finishing up projects described in the previous quarterly report.

INTERNAL CONVERSION ANGULAR CORRELATIONS

M. E. Rose L. C. Biedenharn
G. B. Arfken

This work is now complete. It has been shown that if the angular correlation function for gamma rays and any other radiation x is given by

$$W_{\gamma-x}(\theta) = \sum_{\nu} A_{\nu} P_{\nu}(\cos \theta),$$

where Legendre polynomials are represented by P_{ν} , then the angular correlation between a conversion electron and the radiation x is

$$W_{e-x}(\theta) = \sum_{\nu} b_{\nu} A_{\nu} P_{\nu}(\cos \theta).$$

The radiation x can be another gamma ray, an alpha particle, a beta particle or another conversion electron. In the latter case, $A_{\nu} = b_{\nu} A_{\nu}(\gamma-\gamma)$, where the two b_{ν} 's refer to each conversion electron (they depend on Z , transition energy, parity, and multipolarity), and $A_{\nu}(\gamma-\gamma)$ are the $\gamma-\gamma$ coefficients. The latter have been extensively tabulated. The present work gives the numerical values of the b_{ν} coefficients (relativistically) for K -shell conversion in the range

$$10 \leq Z \leq 96, \quad 0.3 \leq k \leq 5.0,$$

where $k mc^2$ is the transition energy, and for five electric and five magnetic multipoles. A manuscript has been

submitted to *The Physical Review* and numerical tables also appear in an ORNL report.⁽¹⁾

ONE-THREE GAMMA-GAMMA ANGULAR CORRELATION

G. B. Arfken M. E. Rose
L. C. Biedenharn

Whenever three gamma rays occur in cascade it is useful, as a check on double correlation between successively emitted gammas and to resolve possible ambiguities in the interpretation of the level scheme, to measure the correlation between the first and third gamma rays, ignoring the intermediate one. Tables giving the relevant coefficients for $W(\theta)$ expanded in P_{ν} 's have been prepared.⁽²⁾

RACAH COEFFICIENT TABULATION

L. C. Biedenharn

This work is almost completed and will appear in an ORNL report⁽³⁾ to be issued in the near future.

NUCLEAR POLARIZATION AND ALIGNMENT

A. Simon M. E. Rose
J. M. Jauch

Four distinct methods have been proposed for the polarization or alignment of nuclei. Polarization, which is the production of a net

⁽¹⁾M. E. Rose, L. C. Biedenharn, and G. B. Arfken, *Tables of Coefficients for Internal Conversion Angular Correlations*, ORNL-1097 (Sept. 20, 1951).

⁽²⁾G. B. Arfken, L. C. Biedenharn, and M. E. Rose, *One-Three Gamma-Gamma Angular Correlation*, ORNL-1103 (Oct. 30, 1951).

⁽³⁾L. C. Biedenharn, *Tables of the Racah Coefficients*, ORNL-1098.

magnetic moment of the nuclei is accomplished by either the direct action of an external magnetic field⁽⁴⁾ or by the combined action of this field with the nuclear hyperfine structure.^(5,6) Alignment, which produces a change in the nuclear second moment from the isotropic value but creates no first moment, is accomplished by use of an anisotropy hyperfine structure in a paramagnetic salt^(7,8) or by use of the nuclear quadrupole coupling with the crystalline field.⁽⁹⁾

The leading term has been obtained of an expansion of the expression for the nuclear polarization (or alignment) in powers of α/kT where α is a parameter that is small compared to kT . This has been done for all four methods. In particular, for the nuclear polarization with hyperfine structure coupling, it was shown that the entire effect of arbitrary interelectronic interactions is contained in their effect on the electronic susceptibility. There is considerable evidence that magnetic dilution is not necessary for the success of this type of experiment.⁽¹⁰⁾

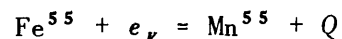
Computation of higher-order terms is complicated by the noncommutativity of various parts of the Hamiltonian. A general method has been derived that allows these terms to be computed to any order and in closed form. This

technique has been applied to several cases of interest. A paper on this subject has been submitted to *The Physical Review*.

INNER BREMSSTRAHLUNG IN BETA DECAY

J. M. Jauch*

The radiative processes accompanying beta transitions were examined theoretically. It is shown that for β^- and β^+ emission and K -capture the probability for the process is independent of the coupling type. In the case of β^- , β^+ emission the photon has a strong angular correlation with the outgoing particle giving a maximum intensity near the forward direction. This angular dependence also is independent of the coupling for allowed transitions. The K -capture inner bremsstrahlung is of special interest insofar as it allows a simple and convenient method for determining the total energy release in the capture process. It is possible to make a plot analogous to a Kurie plot for the photon spectrum leading to a precise determination of the end point. The method was applied by P. R. Bell and J. M. Cassidy to the case of Fe^{55} and the energy release in the process



was determined to be $Q = 206$ kev.

THE TRIPLET FORCE BETWEEN LIKE NUCLEONS

F. C. Prohammer T. A. Welton

A variational calculation has been made for the binding energy of two neutrons and a proton in the quartet state. Such a calculation should yield information on the (n - n) interaction in the triplet state. The two

(4) F. E. Simon, "Le Magnetisme," Conference at Strasbourg, May 1939.

(5) M. E. Rose, "Scattering and Absorption of Neutrons by Polarized Nuclei," *Phys. Rev.* 75, 213 (1949).

(6) C. J. Gorter, "A New Suggestion for Aligning Certain Atomic Nuclei," *Physica* 14, 504 (1948).

(7) B. Bleaney, "On the Spatial Alignment of Nuclei," *Proc. Phys. Soc. (London)* A64, 315 (1951).

(8) B. Bleaney, "Hyperfine Structure in Paramagnetic Salts and Nuclear Alignment," *Phil. Mag.* 42, 441 (1951).

(9) R. V. Pound, "On the Spatial Alignment of Nuclei," *Phys. Rev.* 76, 1410 (1949).

(10) For a contrary opinion see reference (8).

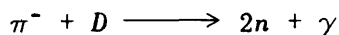
*Summer visitor, University of Iowa.

PHYSICS DIVISION QUARTERLY PROGRESS REPORT

(n - p) interactions were so chosen as to give the correct triplet scattering length and effective range, and the (n - n) interaction was assumed to be zero. Three parameters were used in the trial function, and adjusted to give a minimum value for the energy.

The variational method gives an upper estimate on the energy of the lowest state, and by properly choosing the three parameters in the trial function the lowest upper estimate with that trial function is obtained.

Although the calculation has not been completed, the present upper estimate on the energy is 4.5 Mev, which indicates a virtual state. It is expected that with the optimum choice of parameters this energy will be lower, perhaps zero or perhaps even slightly negative. This preliminary result indicates that whether the (n - n) interaction is attractive or repulsive the magnitude of the interaction is small. This is in agreement with the conclusion of Christian and Noyes⁽¹¹⁾ for the (p - p) triplet interaction, provided the mirror nuclei argument is accepted. The present result of 4.5 Mev, and particularly an expected lower final value, tends to agreement with experimental work of Aamodt, Pauofsky, and Phillips,⁽¹²⁾ who, in studying the



(11) R. S. Christian and H. P. Noyes, "The Proton-Proton Interaction," *Phys. Rev.* 79, 85 (1950).

(12) R. L. Aamodt, W. K. H. Panofsky, and R. Phillips, " π^- Absorption in D_2 and the n - n Force," *Phys. Rev.* 83, 1057 (1951).

process, have found the nominal value of the lowest state of the (n - n) system to be virtual with an energy of 1.2 Mev.

ANGULAR CORRELATION IN NEUTRON DECAY

L. C. Biedenharn D. Beard*

The computation of the angular correlation between recoil proton and β^- in the neutron decay has been finished. The result is that there appears to be a fair possibility of obtaining direct information on the choice of beta interaction from an angular correlation experiment. An ORNL report is being prepared.

DETECTION OF CIRCULARLY POLARIZED GAMMA RAYS

D. Beard M. E. Rose

In a previous report⁽¹³⁾ it was shown that when polarized neutrons are captured by (unpolarized) nuclei the resulting capture gamma rays are circularly polarized. By observing the asymmetry of Compton scattered radiation from magnetized iron the effect could be detected and information on nuclear levels obtained. Unfortunately the asymmetry is much too small from the point of view of performing a successful experiment.

*Summer visitor, Catholic University.

(13) L. C. Biedenharn, M. E. Rose, and G. B. Arfken, "Polarization of Gamma Radiation Following Capture of Polarized Neutrons," *Phys. Rev.* 83, 683 (1951).